Development of a spray evaporation model for SRM simulations

Bachelor thesis

Faculty of Science, Lund University

Thommie Nilsson
Supervisor: Karin Fröjd

Abstract

A fuel vaporization model has been developed for stochastic reactor simulations of engine in-cylinder combustion. The model includes calculations of evaporation rate from fuel droplets based on the diffusion of vapor from the surface of droplets, and the heating of droplets based on convective heat transfer with correction due to mass transfer. A simple deceleration model for droplets was also included. Some of the stochastic particles that represent the cylinder gas were used to represent different parts of the spray and the droplets interact with them in sequence. Dependence on some modeling parameters was investigated and a comparison with an experimental case was also made. The comparison gave qualitatively plausible results.

Table of Contents

Nomenclature

Symbols

A	Base area of a cone, nozzle hole area [m]
C	Specific heat capacity [J/kg]
D	Diameter [m]
D_{32}	De Brouke mean diameter [m]
D_{43}	Sauter mean diameter [m]
D_{ref}	Rosin-Rammler reference diameter [m]
$\mathcal{D}_{AB}$	Diffusivity of gas mixture A into gas mixture B [m^2/s]
d	Distance traveled [m]
f	Distribution function [m^2]
f_t	Distribution function at time t [m^2]
h	Particle length in spray cone [m], heat transfer number [$W/m^2 \cdot K$]
H	Enthalpy [J]
k	Evaporation constant [m^2/s]
k_m	Heat conductivity [W/mK]
K	Time-integral of evaporation constant [m^2]
L	Latent heat of vaporization [J/kg]
m	Droplet mass [kg]
$\dot{m}$	Evaporation rate [kg/s]
$\dot{M}$	Momentum flux [$kg \cdot m/s^2$]
n	Number of spray cones
N	Number of species, number of steps
N_F	Number of fuel species
Nu	Nusselt number
P	Pressure [Pa]
P_{sat}	Saturation vapor pressure [Pa]
Pr	Prandtl number
Q	Transferred power [W]
r	Radius of spray cone [m]
R	Radius of effective spray cone [m]
Re	Reynolds number
t	Time [s]
T	Temperature [K]
v	Droplet velocity [m/s]
V	Droplet volume, particle volume [m^3]
X	Mole fraction
Y	Mass fraction
z	Correction factor

Greek symbols

α	Gaussian shape parameter
δ	Rosin Rammler shape parameter
φ	Effective spray opening angle
μ	Viscosity [Pa·s]
ρ	Density [kg/m^3]
θ	Spray opening angle

Subscripts

∞	At infinite distance
0	Initial condition
avg	Average value
d	Droplet
f	In droplet film
F	Gas belonging to droplet
l	Liquid
G	Gas belonging to particle
g	Surrounding gas
p	At constant pressure
s	At droplet surface
v	Pure fuel vapor

1 Introduction

1.1 The stochastic reactor model

A stochastic reactor model (SRM) is a physics-based, zero-dimensional (no spatial resolution) model involving random numbers which is used for simulation of chemical reaction systems. In this work, the model considered is DARS SRM for in-cylinder combustion simulation, and the aim of the project is to develop a fuel vaporization model and implement it into the existing code.

The basic principle of the SRM is that the mass in the system (the cylinder) is split into a number of "particles", each with its own temperature, density and mass fractions. The model uses operator splitting: for each time step the pressure-volume work, fuel injection, mixing of particles, chemical reactions and heat transfer are solved independently in sequence (see Figure 1). The chemical reactions and heat transfer are solved independently for each particle while the piston movement is solved globally (the pressure is assumed constant throughout the cylinder). The model can be described by a partial differential equation of the form

$$\frac{\partial}{\partial t}F_{\Phi}(\psi,t)+\frac{\partial}{\partial \psi_i}\Big(Q_i(\psi)F_{\phi}(\psi)\Big)=mixing\ term \qquad (1)$$

where F_{Φ} is a probability density function (PDF) describing the system, ψ_i represent all variables used in that description, t is time and Q_i is the change in variable i due to processes like chemical reaction and heat losses. $mixing\ term$ represent an expression for the change due to mixing.

In the mixing step the particles exchange gas with each other. Particles are chosen randomly in pairs and mixed completely to their common mean. How often mixing occurs is controlled by the mixing time τ which in general is time-dependent. τ is a measure of the turbulence intensity in the gas and represent the average time it takes for a particle before it is mixed. The definition is [1]

$$\tau=\frac{l_I}{\overline{U}} \qquad (2)$$

where l_I is the integral length scale of the flow field and $\overline{U}$ is the mean gas velocity.

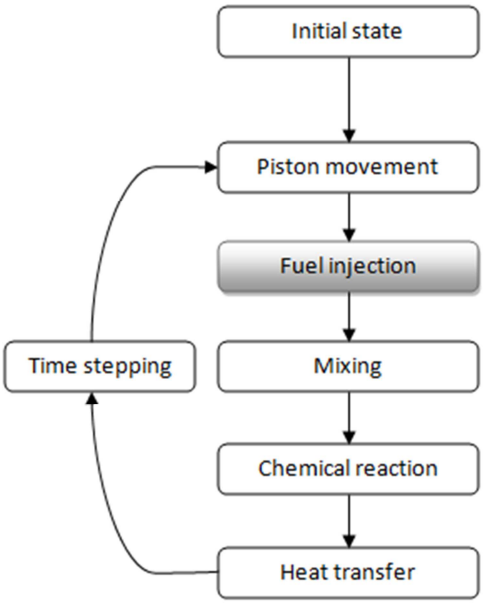

Figure 1 Schematic picture of the operator split loop.

Since the model is zero-dimensional there is no information on the spatial distribution of gas and temperature. An alternative approach is to divide the cylinder volume into small cells and then to solve the gas flow between cells in every time step (computational fluid dynamics, CFD). This approach gives the spatial resolution but at the cost of more CPU time; the advantage of SRM is computational efficiency.

1.2 Problem formulation

The aim is to calculate the rate of vaporization of a fuel spray, i.e. how much fuel is vaporized during each time step. The current implementation uses a pre-calculated or fitted vaporization curve as input, mixes the injected fuel with an appropriate amount of existing cylinder gas to reach vaporization temperature and then adds the mixture in form of a new particle. A vaporization model is motivated for two reasons: First, it reduces the complexity of the input parameters since it will use the easier available injection curve instead of a vaporization curve. Secondly, it allows the vaporization rate to depend on the modeling conditions in the cylinder and thus also to vary from cycle to cycle because of stochastic effects and exhaust gas recycling (EGR).

The rate of injection into the cylinder depends on the pressure in the injector and on the size and shape of the nozzle. That is not modeled here since this work is restricted to the fuel vaporization, so instead a pre-defined mass injection profile is used. Wetting of the cylinder walls is also left out.

Another aim is not to just calculate the vaporization rate but also to distribute the vaporized mass among the existing particles in a way that represents how injected fuel is actually distributed.

2 Model description

In short, the method is as follows: A few particles are selected to represent the space close to the injector. The fuel travels through the volume of these particles and for every time step the evaporation, heating and velocity is calculated for the fuel droplets. These selected particles receive the evaporated mass and are cooled by the droplet heating.

2.1 Liquid parcels and the particle queue

At each time step some fuel is injected according to the injection profile. The fuel consists of a spray of small droplets spreading like a cone. The injected fuel is divided into parcels (analogous to the gas particles). Each parcel represents an ensemble of physical droplets of various sizes. The distribution of droplet sizes within a parcel is given by a PDF which is initially assumed to be a Rosin-Rammler distribution function (other reasonable choices could have been the logarithmic distribution function, the upper-limit distribution or the Nukiyama-Tanasawa distribution, see for example [1] and [2] p523). The Rosin-Rammler distribution is given by

$$f_{RR}(D) \propto D^{\delta-1} e^{-\left(\frac{D}{D_{ref}}\right)^{\delta}} \tag{3}$$

where δ is a shape parameter and D_{ref} is a reference diameter (the volume average); both are related to the Sauter and De Brouke mean diameters D_{43} and D_{32} by [3]

$$\left(D_{jk}\right)^{j-k} = \left(D_{ref}\right)^{j-k} \frac{\Gamma\left(\frac{j-3}{\delta}+1\right)}{\Gamma\left(\frac{k-3}{\delta}+1\right)} \tag{4}$$

Figure 2 shows the Rosin-Rammler distribution for $D_{ref} = 3$ μm and $\delta = 2$.

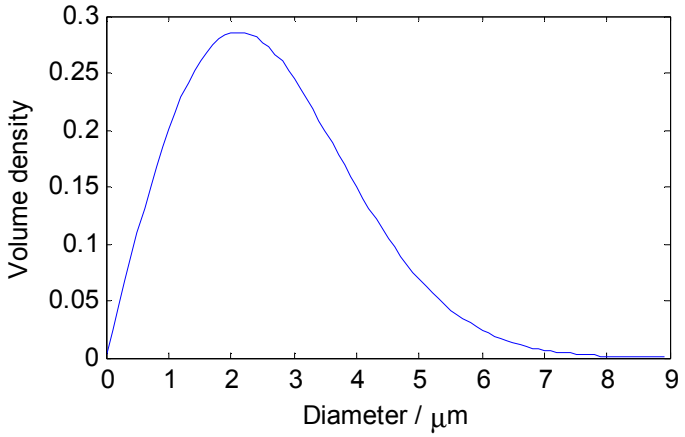

Figure 2. Rosin-Rammler distribution.

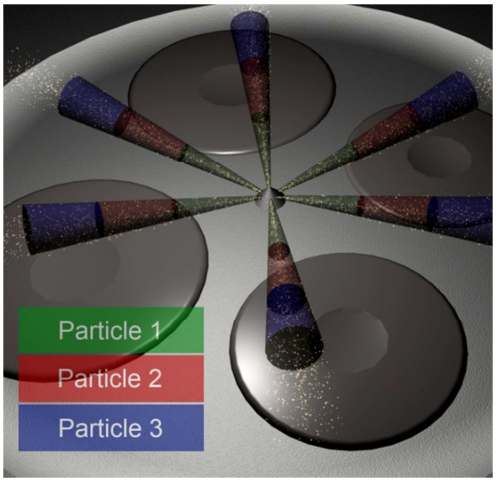

Figure 3. Particle representation of the space occupied by the spray.

The distribution function $f(D)$ describes the volume density, $f(D) = \frac{dV}{dD}$, so that $f(D)dD$ is the volume contained in droplets in the diameter interval dD. $f_0(D)$ is normalized so that its integral is equal to the initial volume. When distributions at other times than the initial occur, these will be denoted $f_t(D)$ and be normalized for the volume remaining at that time. The droplet diameter distribution is used mainly for the evaporation calculation. For the heating an effective average diameter is used.

For a multi-component fuel the parcels are divided into compartments, one per fuel, and these compartments have their own distributions, which mean that the fuel components are assumed to evaporate independently.

The only properties of the parcels that are modeled in this work are diameter distribution, temperature, mass fractions, mass, travelled distance and velocity. Thus, things like droplet density, dissolution of gas in droplets and liquid chemistry are not considered. It is also assumed that the temperature, velocity and spatial position are the same for all droplets within a parcel, i.e. independent of droplet diameter. All parcels are treated independently, one at a time, and there is assumed to be no interaction between droplets (like collisions) except indirectly via the gas particles.

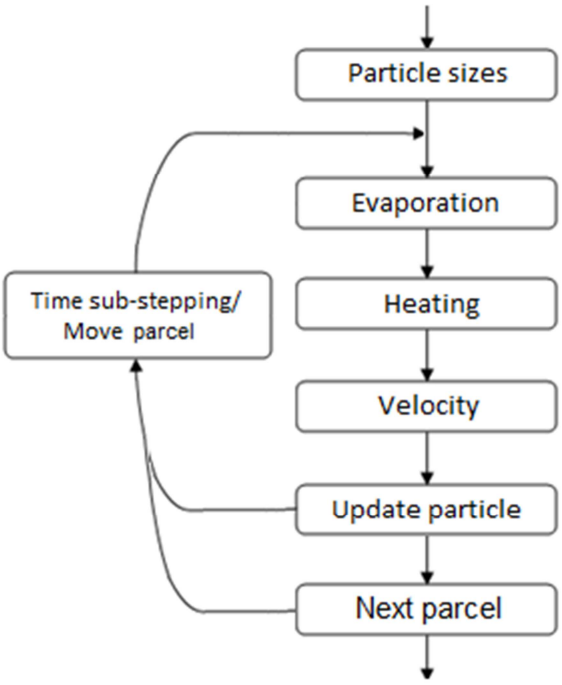

Figure 4 The vaporization calculations.

To represent the space occupied by the spray, a set of gas particles are chosen and given a spatial interpretation (see Figure 3). The parcels travel from particle to particle in a straight line in this order, and interact with the particle it is currently in. Some particles will interact more with the parcels than others based on what part of the spray they represent, giving an uneven distribution of fuel vapor among the particles.

During a time step Δt a parcel travels a distance $d = v \cdot \Delta t$ which may or may not be in the same particle. If the parcel travels through more than one particle then the time step is split into smaller sub steps, one for each particle. Also, to compensate for the fact that fuel is injected continuously during the time step when a parcel is created, the first time step is halved for that parcel to get an average.

2.2 The structure of the model

The calculations of the model are illustrated in Figure 4.The particle sizes (see below) are calculated only once per global time step, they are assumed not to change size significantly during a step due to the addition of evaporated mass. The rest of the calculations are performed for one parcel at a time and in smaller sub-steps. The evaporation is solved first and for one fuel species at a time (but without changing any parameters between the species). Secondly the heating is solved followed by a velocity calculation. After these calculations are done the evaporated mass is added to the particle and the particle enthalpy is adjusted.

2.3 Representing the spray cone

In order to find the time it takes for a parcel to pass through a particle every particle must have a length assigned to it. The particle lengths are determined by treating the spray as a cone with each particle being a segment of it (a truncated cone) with the appropriate volume. The height of a cone as function of volume and angle is given by:

$$V = \frac{\pi}{3} r^2 \cdot h = \frac{\pi}{3}\left(h \cdot \tan\left(\frac{\theta}{2}\right)\right)^2 h \Leftrightarrow h = \left(\frac{3V}{\pi \cdot \tan^2\frac{\theta}{2}}\right)^{1/3} \tag{5}$$

where θ is the opening angle, r is the base radius and V is the volume of the cone. If V_i is the volume of particle number i in the queue, V_0 and h_0 are the total volume and length of all particles before it and h is the length of the full cone up to and including particle i, then the length of particle i is the difference

$$h_i = h - h_0 = \left(\frac{3(V_i + V_0)}{\pi \cdot \tan^2\frac{\theta}{2}}\right)^{1/3} - \left(\frac{3V_0}{\pi \cdot \tan^2\frac{\theta}{2}}\right)^{1/3} \tag{6}$$

Also the first particle is treated as a truncated cone since the nozzle hole has a finite area A; this corresponds to removing the tip of the spray cone. The height of that tip is

$$h_{tip} = \frac{r}{\tan\left(\frac{\theta}{2}\right)} = \frac{\sqrt{A/\pi}}{\tan\left(\frac{\theta}{2}\right)} \tag{7}$$

The opening angle θ of the spray is an input parameter, but in general there is more than one spray cone. In that case, a larger, effective cone is of the same length h and total volume V as the individual cones, but with a new effective opening angle φ, is used instead. A segment of the new cone has base radius R. If n is the number of cones and V_j is the volume of a segment of one cone then φ is given by

$$n \cdot V_j = V \Leftrightarrow n \cdot \frac{\pi}{3} h r^2 = \frac{\pi}{3} h R^2 \Leftrightarrow \; n \cdot r^2 = R^2 \Leftrightarrow \tag{8}$$

$$n \cdot \left(h \cdot \tan\left(\frac{\theta}{2}\right)\right)^2 = \left(h \cdot \tan\left(\frac{\varphi}{2}\right)\right)^2 \Leftrightarrow \tan\left(\frac{\varphi}{2}\right) = \sqrt{n} \cdot \tan\left(\frac{\theta}{2}\right) \Leftrightarrow$$
$$\varphi = 2 \cdot \arctan\left(\sqrt{n} \cdot tan\left(\frac{\theta}{2}\right)\right)$$

The effective φ is used only to get the lengths right and does not represent a physical cone width.

2.4 Evaporation

The vaporization rate is assumed to depend only on the rate of diffusion of vapor into the surrounding gas, which is true for a dense spray [4]. The diffusion is described by the D^2-law (derived from Fick's law of diffusion) [5], $\frac{d(D^2)}{dt} = -k$ where D is the droplet diameter and k is the evaporation constant:

$$k = \frac{8\rho_g \mathcal{D}_{AB}}{\rho_l} \ln \frac{1 - \mathrm{Y_{A,\infty}}}{1 - Y_{A,s}} \tag{9}$$

In this expression, ρ_l and ρ_g are the densities of the liquid droplet and surrounding gas respectively and $\mathcal{D}_{AB}$ is the diffusivity of fuel vapor A from the film close to the droplet surface into the surrounding gas B of the particle. $Y_{A,\infty}$ and $Y_{A,s}$ are the mass fractions of fuel vapor far away from the droplet and in the film close to the droplet surface, respectively. Far away, the mass fraction $Y_{A,\infty}$ is taken to be that of the gas particle. The mass fraction in the film is described later.

The D^2-law describes the rate of change of the squared droplet diameter. It follows that

$$\frac{d(D^2)}{dt} = \frac{d(D^2)}{dD} \cdot \frac{dD}{dt} = -k \Leftrightarrow 2D \cdot \frac{dD}{dt} = -k \Leftrightarrow \frac{dD}{dt} = -\frac{k}{2D} \tag{10}$$

The time-dependence of the diameter D is thus, in a sufficiently small time interval where k can be assumed constant,

$$2D \cdot \frac{dD}{dt} = -k \Leftrightarrow [D(t')^2]_0^t = -\int_0^t k dt' = -kt \Leftrightarrow D^2(t) = D_0^2 - kt$$
$$\Leftrightarrow D(t) = \sqrt{D_0^2 - kt} \quad \text{or} \quad D_0 = \sqrt{D(t)^2 + kt} \tag{11}$$

D_0 is the diameter at time 0 that correspond to diameter D at time t. This can also be used as a recursive formula for $D(t + \Delta t)$ when $D(t)$ is known:

$$D_{i+1} = \sqrt{D_i^2 - k\Delta t} = \sqrt{D_0^2 - \sum_{j=1}^{j=i-1} k_j \Delta t} \tag{12}$$

In the second expression the evaporation constant has been written as a step function. From the above it also follows that

$$\frac{dD_0}{dD} = \frac{D}{\sqrt{D^2 + kt}} \tag{13}$$

The D^2-law describes the behavior of a single droplet, but the aim is to find the time evolution of the entire size distribution. One way of doing this is to split the diameter range into a series of sections (size classes) and solve the evaporation for each class individually. Another method is to assume that the evaporation constant k is independent of droplet diameter, which is true if all droplets have the same temperature, to make an exact solution is possible; this is the method used in this work. Also, since different species are treated separately (they have different k), every species will have its own distribution, volume and mass.

The volume of the droplets in a small range ΔD_i centered D_i at is $V_i \approx f(D_i)\Delta D_i$ where $f(D)$ is the volume density (Rosin-Rammler distribution) of the parcel. The number of droplets in such a range is conserved (they evaporate at the same rate and start at the same diameter) and is given by the total volume of all droplets in the range divided by the volume of a single droplet at any given time:

$$n_i = \frac{V_i}{V_{droplet}} = \frac{V_i}{\frac{\pi}{6}D_i^3} = \frac{V_{0,i}}{\frac{\pi}{6}D_{0,i}^3} \tag{14}$$

where $V_{0,i}$ and $D_{0,i}$ is the volume and diameter at time $t = 0$. This gives a useful expression for how the volume distribution (volume density) is related to the number distribution:

$$N(D) = \frac{dn}{dD} = \frac{d}{dD}\left(\frac{V}{V_{droplet}}\right) = \frac{\frac{dV}{dD}}{V_{droplet}} = \frac{f(D)}{\frac{\pi}{6}D^3} \tag{15}$$

Note that the derivative is taken with respect to diameters in the distribution (the position of the range ΔD); the volume of one droplet at any given diameter position is just a constant parameter.

2.4.1 Film mass fractions

To find an expression for the film mass fraction $Y_{A,s}$ appearing in the evaporation constant, the film close to the droplet surface is assumed to have a partial pressure of fuel P_{film} given by a weighted average of the partial pressure in the surrounding gas (the particle) P_∞ and the saturation vapor pressure P_{sat}, $P_{film} = \frac{2P_{sat}+P_\infty}{3}$ [6]. A lower vapor pressure (non-saturation) can be simulated simply by multiplying the saturation vapor pressure by a factor corresponding to the relative saturation.

If the fuel consist of only one species (denoted by i) and the global pressure in the cylinder is P then the mole fraction of fuel vapor at the surface is

$$X_i = \frac{P_f}{P} \tag{16}$$

If the film partial pressure at some point is larger than the global pressure (which can happen in the simulation if the critical temperature is reached) then X_i is set to 1. The gas mixture at the droplet surface can be divided into two components: fuel vapor (belonging to the droplet) and residual gas (belonging to the gas particle). Let X_F and X_G be the mole fractions of fuel vapor and residual gas respectively, with $X_G + X_F = 1$. If $X_{G,i}$ is the mole fraction of the fuel species already present in the residual gas, then

$$X_i = X_F + X_G \cdot X_{G,i} \tag{17}$$

Use of $X_F = 1 - X_G$ gives

$$X_i = 1 - X_G + X_G \cdot X_{G,i} \Leftrightarrow X_G = \frac{X_i - 1}{X_{G,i} - 1} \tag{18}$$

To be able to convert the mole fractions into mass fractions, the mole fractions of all species present must be known. For the gas species that are not fuel, the mole fractions are now given by $X_j = X_{G,j} \cdot X_G$ and for the fuel species it is $X_i = \frac{P_f}{P}$. From these mole fractions and the molecular weights all the mass fractions can be calculated, in particular $Y_{A,s}$.

For multi-component fuels the partial pressure of one of the fuel species in saturated gas is, according to Raoult's law [7], the saturation pressure of that species times the mole fraction in

the liquid of that species, $P'_{sat,i} = P_{sat,i}X_{\ell,i}$ where $X_{\ell,i}$ is the mole fractions in the liquid phase and $P_{sat,i}$ is the saturation vapor pressure of species i. The partial pressure in the film of any fuel species is then, with the averaging, $P_i = \frac{2P'_{sat,i}+P_{\infty,i}}{3}$ where $P_{\infty,i}$ is the partial pressure of species i in the particle. This gives the desired mole fractions for any fuel species via the global pressure P:

$$X_i = \frac{P_i}{P} = \frac{\left(2P'_{sat,i} + P_{\infty,i}\right)/3}{P} \tag{19}$$

The mole fractions for non-fuel species are needed as well. Let X_F be the mole fraction of gas belonging to the droplet and X_G the mole fraction of gas belonging to the gas particle. Then $X_{F,i}$ and $X_{G,i}$ are the mole fractions of species i in these parts of the gas. This means that for every non-fuel species:

$$X_j = X_G \cdot X_{G,j} \tag{20}$$

What is needed is X_G. If N_F is the number of fuel species, the total partial pressure of fuel vapor is the weighted sum

$$P_f = \sum_i^{N_F} P_i \tag{21}$$

Let $X_{fuel\ species}$ be the sum of the mole fractions of all fuel vapor (from the particle as well as from the droplet), that is

$$X_{fuel\ species} = \sum_i^{N_F} X_i = \sum_i^{N_F} \frac{P_i}{P} = \frac{P_f}{P} \tag{22}$$

$X_{fuel\ species}$ is also given by

$$X_{fuel\ species} = \underbrace{\sum_i^{N_F} X_{i,F}X_F}_{=X_F} + \sum_i^{N_F} X_{i,G}X_G = X_F + X_G \sum_i^{N_F} X_{i,G} \tag{23}$$

With use of $X_F + X_G = 1$ this gives the expression for X_G:

$$\begin{aligned} X_{fuel\ species} = \underbrace{\sum_i^{N_F} X_{i,F}X_F}_{=X_F} + \sum_i^{N_F} X_{i,G}X_G = 1 - X_G + X_G \sum_i^{N_F} X_{i,G} = \\ = 1 + X_G\left(\sum_i^{N_F} X_{i,G} - 1\right) \end{aligned} \tag{24}$$

$$X_G = \frac{X_{fuel\ species} - 1}{\sum_i^{N_F} X_{i,G} - 1} = \frac{\frac{P_f}{P} - 1}{\sum_i^{N_F} X_{i,G} - 1} \tag{25}$$

2.4.2 Time evolution using size classes

The time evolution of the volume of each size class is found by using the above expressions:

$$V_i(t) = n_i \frac{\pi}{6} \cdot D_i^3(t) \tag{26}$$

This also gives the useful expression

$$\frac{dV(t)}{dn} = \frac{\pi}{6}D^3 \quad \text{and} \quad \frac{dn}{dV_0} = \frac{1}{\frac{\pi}{6}D_0^3} \tag{27}$$

The time-evolved diameter distribution however is obtained by plotting the volume density of each size class against their new median diameter. Since the diameters changes, at a later time the classes are no longer equidistant. To get the volume density of a class its volume must be divided by the proper interval ΔD. these intervals are approximated by

$$\Delta D(t) \approx \frac{dD}{dD_0}\Delta D_0 = \frac{D_0}{\sqrt{D_0^2 - kt}} \cdot \Delta D_0 = \frac{\sqrt{D(t)^2 + kt}}{D(t)} \cdot \Delta D_0 \tag{28}$$

where ΔD_0 is the spacing of the initial diameter intervals.

2.4.3 Time evolution of the continuous distribution

Assuming a diameter-independent evaporation constant (diameter-independent temperature) and using the expressions above gives the exact solution (quantities with subscript 0 are for time 0):

$$f_t(D) = \frac{dV(t)}{dD} = \frac{dV(t)}{dn(V_0)} \cdot \frac{dn(V_0)}{dV_0(D_0)} \cdot \frac{dV_0(D_0)}{dD_0(D)} \cdot \frac{dD_0(D)}{dD} =$$

$$= \frac{\pi}{6}D^3 \cdot \frac{1}{\frac{\pi}{6}D_0^3} \cdot f_0(D_0) \cdot \frac{D}{\sqrt{D(t)^2 + kt}} = \left(\frac{D}{\sqrt{D^2 + kt}}\right)^4 \cdot f_0(D_0)$$

The time-dependent distribution becomes

$$f_t(D) = f_0\left(\sqrt{D^2 + kt}\right) \cdot \frac{D^4}{(D^2 + kt)^2} \tag{30}$$

where f_0 is the distribution at time $t = 0$. A validation of this expression by comparison with the result of a size classes calculation (as described above using 50 classes) was done and it showed good agreement. Figure 5 shows the result of the evaporation formula for a constant k.

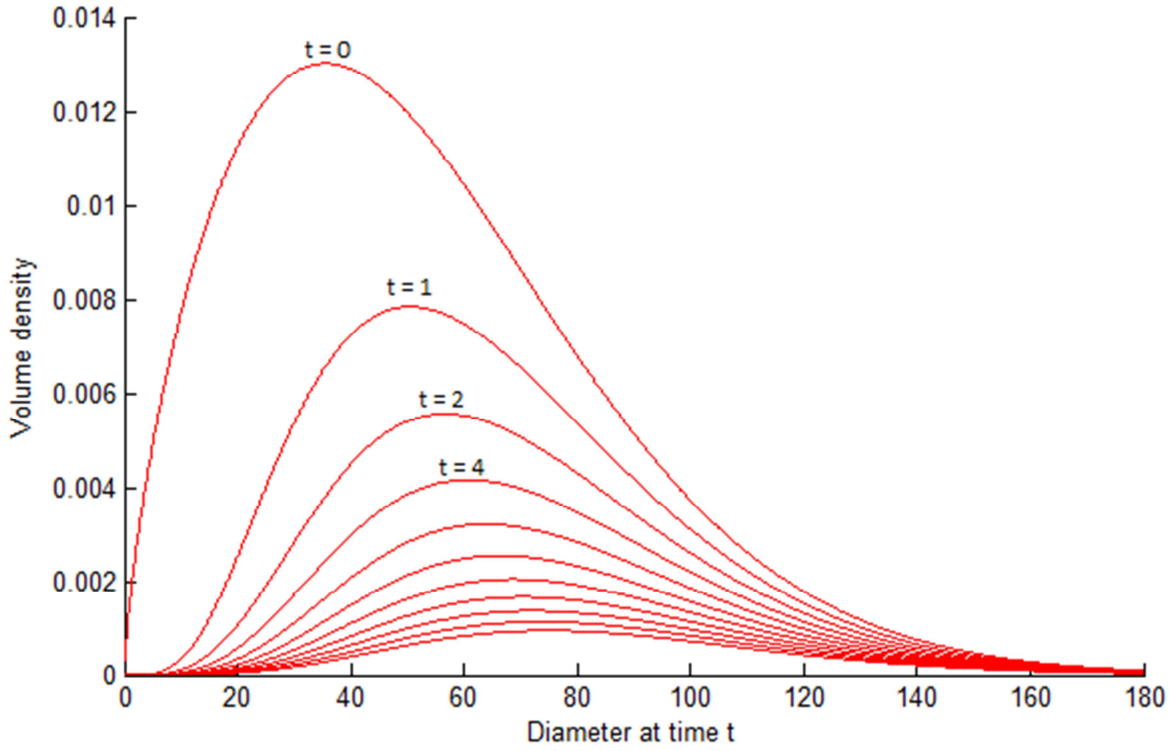

Figure 5. Time evolution of the distribution function (volume distribution).

2.4.4 Time-dependent evaporation constant

Since the droplets travel through a series of gas particles with different properties, the value of the evaporation constant k must be allowed to change with time. Since k only appear as the product kt in the expression derived above, this can be done by the replacement $kt \rightarrow \int_0^t k(t)dt$. This cannot change the shape of the time-evolved distribution, just the rate at which it evolves (i.e. the evaporation rate) and the distribution is

$$f_t(D) = f_0\left(\sqrt{D^2 + \int_0^t k(t)dt}\right) \cdot \frac{D^4}{\left(D^2 + \int_0^t k(t)dt\right)^2} = f_0\left(\sqrt{D^2 + K_t}\right) \cdot \frac{D^4}{(D^2 + K_t)^2}$$

where

$$K_t = \int_0^t k(t)dt \tag{32}$$

In the implementation of the model, $f_{t+\Delta t}$ for a new time step is calculated by

$$f_{t+\Delta t}(D) = f_0\left(\sqrt{D^2 + K_{t+\Delta t}}\right) \cdot \frac{D^4}{(D^2 + K_{t+\Delta t})^2} \tag{33}$$

The value of $K_{t+\Delta t}$ is calculated from

$$K_{t+\Delta t} = \int_0^t k(t)dt + \int_t^{t+\Delta t} k(t)dt = K_t + k(t + \Delta t) \cdot \Delta t \tag{34}$$

where $k(t + \Delta t)$ is assumed to be constant during the time step and calculated as described above. K_t is saved from the previous time step.

2.4.5 Volume and mass

The volume at a time t is found by integrating $f_t(D)$:

$$V(t) = \int_0^{D_{max}} f_t(D)dD \tag{35}$$

The evaporated volume between t and $t + \Delta t$ is

$$\Delta V = V(t) - V(t+\Delta t) = V(t) - \int_0^{D_{max}} f_{t+\Delta t}(D)dD \Leftrightarrow$$

$$\Delta V = V(t) - \int_0^{D_{max}} f_0\left(\sqrt{D^2 + K_{t+\Delta t}}\right) \cdot \frac{D^4}{\left(D^2 + \int_0^{t+\Delta t} k(t)dt\right)^2} dD \Leftrightarrow \tag{36}$$

$$\Delta V = V(t) - V_0 \int_0^{D_{max}} f_0^*\left(\sqrt{D^2 + K_{t+\Delta t}}\right) \cdot \frac{D^4}{(D^2 + K_{t+\Delta t})^2} dD$$

where V_0 is the initial volume of the parcel and f_0^* is the initial distribution normalized to 1. The normalization is done assuming the distribution to be identically zero for diameters larger than $D_{max} = 4D_{ref}$. The evaporated mass is

$$\Delta m = m(t) - \rho_l \cdot V_0 \int_0^{D_{max}} f_0^*\left(\sqrt{D^2 + K_{t+\Delta t}}\right) \cdot \frac{D^4}{(D^2 + K_{t+\Delta t})^2} dD \tag{37}$$

The droplet density ρ_l is assumed to be constant (this is also done in the derivation of the D^2-law [5]); the expansion of droplets due to heating is not modeled. Thus, $\rho_l \cdot V_0 = m_0$.

Since all parcels are created with the same (Rosin-Rammler) initial distribution this means that in this model, the mass of any parcel at any time is completely determined by the integral K_t. The reason for this is the assumption that all droplets in the parcel have the same temperature which leads to a diameter-independent k. To make the calculations more effective it is possible to create a table that relates the fraction of mass remaining directly to K_t and use that instead of calculating the integral every time.

If there is more than one fuel species these calculations are performed for every species separately. Every fuel has its own mass, temperature and K_t.

2.5 Heating

The evaporation constant of the D^2-law is strongly dependent on droplet temperature, mainly by the saturation pressure. Directly after injection the evaporation is typically very slow as the droplet is heated up. When the droplet has become warmer the evaporation goes faster and the evaporation constant approaches a constant value [4], see Figure 6.

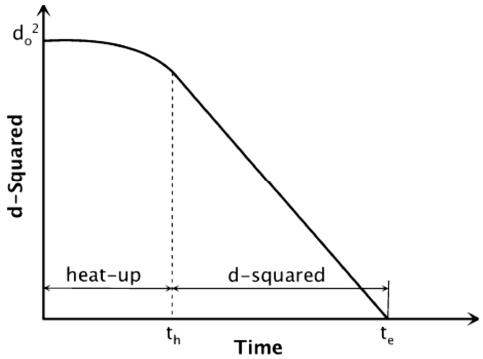

Figure 6 Square diameter against time. Picture borrowed from [3].

2.5.1 Heating of individual droplets

The thermal conductivity of a liquid droplet is assumed infinite so that there is no temperature gradient inside the droplet [8]. Heat transfer by radiation is not modeled. The power transferred to a droplet by convection is [7]

$$Q = \frac{dH}{dt} = A_d h\left(T_g - T_d\right) \tag{38}$$

where H is the droplet enthalpy, A_d is the surface area of the droplet, T_g and T_d are the gas and droplet temperatures and h is the convective heat transfer coefficient. The energy received by the droplet is spent on both heating of the liquid and on vaporization (phase transition). This gives an energy balance to solve [8]:

$$Q_{heat} = Q_{in} - Q_{vap} \tag{39}$$

$$\underbrace{m_d C_{pd}(T_d)\frac{dT_d}{dt}}_{heating\ of\ liquid} = \underbrace{A_d h\left(T_g - T_d\right)}_{enthalpy\ in\ (convection)} - \underbrace{\dot{m}_d L(T_d)}_{vaporization} \tag{40}$$

The rate of evaporation $\dot{m}_d$ is taken to be the same as the rate of diffusion described by the D^2-law. $L(T_d)$ is the latent heat of vaporization at the droplet temperature, C_{pd} the liquid specific heat capacity at constant pressure, m_d the droplet mass and A_d the droplet surface area.

As illustrated by Figure 4, the method is to first calculate the evaporated mass from the D^2-law, use that to solve the energy balance for the enthalpy transferred to the droplet, reduce the transferred enthalpy by the amount needed for evaporation, and then use the remaining enthalpy to heat the liquid mass.

The energy balance can be solved analytically if assuming that the latent heat of vaporization L and the heat capacity C_{pd} are constant. The solution is

$$m_d C_{pd}\frac{dT_d}{dt} = A_d h\left(T_g - T_d\right) + \dot{m}L \Leftrightarrow \frac{dT_d}{dt} + \frac{A_d h}{m_d C_{pd}}T_d = \frac{A_d h T_g + \dot{m}L}{m_d C_{pd}} \Leftrightarrow$$

$$T_d(t) = k \cdot e^{-\frac{A_d h}{m_d C_{pd}}\cdot t} + \frac{A_d h T_g + \dot{m}L}{m_d C_{pd}}$$

$$T_d(0) = T_{d0} \Leftrightarrow k = T_{d0} - \frac{A_d h T_g + \dot{m}L}{m_d C_{pd}} \Rightarrow \tag{42}$$

$$T_d(t) = \left(T_{d0} - \frac{A_d h T_g + \dot{m}L}{m_d C_{pd}}\right) \cdot e^{-\frac{A_d h}{m_d C_{pd}}\cdot t} + \frac{A_d h T_g + \dot{m}L}{m_d C_{pd}} \tag{43}$$

If L and C_{pd} are not constant a numerical method has to be used; in this work an iterative method. For a time step Δt, which is smaller than the global time step, the transferred enthalpy is calculated by

$$\begin{aligned} \Delta H_d &= Q_{heat}\Delta t = \left(Q - Q_{evap}\right)\Delta t \Leftrightarrow \\ \Delta H_d &= A_d h\left(T_g - T_d\right)\Delta t - \dot{m}L(T_d)\Delta t \end{aligned} \tag{44}$$

The temperature change is

$$\Delta T_d = \frac{\Delta H_d}{m_d C_{pd}} \tag{45}$$

The iterative procedure for N steps is thus

$$H_d^{n+1} = H_d^n + \Delta H_d^n = H_d^n + \left(A_d h\left(T_g - T_d^n\right) - \dot{m}L(T_d)\right)\cdot\frac{\Delta t}{N} \tag{46}$$

$$T_d^{n+1} = T_d^n + \Delta T_d^n = T_d^n + \frac{A_d h\left(T_g - T_d^n\right) - \dot{m}L(T_d)}{m_d C_{pd}}\cdot\frac{\Delta t}{N} \tag{47}$$

After every step of iteration, the surrounding gas (the particle) is updated by the removing ΔH_d from its enthalpy, the droplet is updated by changing its temperature and L and C_{pd} are recalculated for the new temperatures.

The heat transfer coefficient h is related to the Nusselt number [7] by definition:

$$h = \mathrm{Nu}\frac{k_m}{D_d} \tag{48}$$

where k_m is the thermal conductivity of the gas film surrounding the droplet and the characteristic length scale is set to be the droplet diameter D_d. To calculate h the method described by El Wakil [8] is used: First h is calculated for pure convection with no net mass transfer. Then it is multiplied by a reducing correction factor due to evaporation of mass from the droplet giving

$$h = \mathrm{Nu}\frac{k_m}{D_d}\cdot\frac{z}{e^z - 1} \tag{49}$$

where

$$z = \frac{wC_{pf}}{\pi D_d^2 h} = \frac{-\dot{m}_d C_{pf}}{\pi D_d k_m \mathrm{Nu}} \tag{50}$$

In this expression, $w = -\dot{m}_d$ denotes the rate at which vapor leaves the droplet and C_{pf} is the specific heat capacity of pure fuel vapor in the film. D_d and m_d are droplet diameter and mass. The Nusselt number is calculated as [6]

$$\mathrm{Nu} = 2 + 0.6\cdot \mathrm{Re}^{1/2}\cdot \mathrm{Pr}^{1/3} \tag{51}$$

where Re and Pr are Reynolds and Prandtl numbers for the gas film, given by

$$\mathrm{Pr} = \frac{C_{pf}\mu_f}{k_{m,f}}\ , \qquad \mathrm{Re} = \frac{\rho_g v_d D_d}{\mu_f} \tag{52}$$

μ_f, $k_{m,f}$ and C_{pf} are viscosity, heat conductivity and heat capacity of the film, v_d is the velocity of the droplet relative to the surrounding gas (assumed stationary) and ρ_g is density of the surrounding gas. The film viscosity, heat conductivity and heat capacity are estimated by weighted averages similar to the ones used for the partial pressures [6]:

$$\mu_f = \left(\frac{2P_{v,s} + P_{v,\infty}}{3P}\right)\mu_v(T_f) + \left(1 - \frac{2P_{v,s} + P_{v,\infty}}{3P}\right)\mu_g(T_f) \tag{53}$$

$$k_{m,f} = \left(\frac{2P_{v,s} + P_{v,\infty}}{3P}\right)k_{m,v}(T_f) + \left(1 - \frac{2P_{v,s} + P_{v,\infty}}{3P}\right)k_{m,g}(T_f) \tag{54}$$

$$C_{p,f} = \left(\frac{2P_{v,s} + P_{v,\infty}}{3P}\right)C_{p,v}(T_f) + \left(1 - \frac{2P_{v,s} + P_{v,\infty}}{3P}\right)C_{p,g}(T_f) \tag{55}$$

where the indices v and g means pure fuel vapor and surrounding gas, respectively. The film temperature T_f is estimated by [6]

$$T_f = \frac{1}{3}T_g + \frac{2}{3}T_d \tag{56}$$

An important point is that the fuel composition for which the physical properties are evaluated do not have to be the same as that used by the chemistry solver. The choice of fuel for the chemistry, e.g. pure n-heptane to simulate diesel, is based on combustion properties like ignition point and soot formation, but not on the physical properties used in heating and evaporation calculations. Thus these calculations should be performed with a separate set of fuel properties for better accuracy. For example, in lack of data for actual diesel fuel, dodecane is a better substitute than n-heptane for physical properties [10].

2.5.2 Heating of a parcel

In this model all droplets in a parcel are assumed to have the same temperature. The volume distribution is used to find the volume average droplet diameter D_{avg} (for a multi-component

fuel the distributions for different species are first added together, weighted with their relative masses) and average droplet mass m_{avg} of a parcel. The heat transfer coefficient and surface area are calculated for the average droplet, the area is multiplied by $\frac{m_{droplet}}{m_{avg}}$ and then this is used to calculate the heating of the entire parcel mass. For the evaporation rate in the correction factor, z, the evaporation rate for an average droplet is used: $\dot{m}_{avg} = \dot{m}_{tot} \cdot \frac{m_{avg}}{m_{droplet}}$.

It is also possible to use the distribution to calculate the full area of all droplets in a parcel, but use of this area for the heating (under the assumption that all droplets have the same temperature) gives unphysical results. Most of the area belongs to small droplets while most of the mass belongs to droplets close to D_{avg} (small droplets have larger area/volume ratio). This means most of the area should only be used to heat a small fraction of the parcel mass while the rest of the mass should be heated by a much smaller. Use of the entire area would therefore give too fast heating.

Since large droplets should heat slower than the average these should take longer to evaporate, and the other way around for small droplets. This is expected to be one of the largest limitations of this model. Also, the use of the volume average as a representative diameter is an approximation based on where most of the mass is. For the possibility to tune the heating model separately to experimental observations, the volume average diameter D_{avg} is multiplied by a freely variable parameter. Changing this parameter only affects the heating calculation, unlike changing D_{ref} which also affects the evaporation calculations.

Another feature added to the heating model is to stop the heating as soon as the critical temperature is reached (for single-component fuels). When this happens the heating is considered to be done and the evaporation is governed only by diffusion.

2.6 Velocity

The initial velocity of a droplet is estimated directly from the rate of injected mass and the nozzle hole area A. During a time step Δt the volume V is injected giving $v_0 = \frac{V}{A \cdot \Delta t} = \frac{m/\rho}{A \cdot \Delta t}$.

The entire parcel is assumed to have the velocity of a single droplet traveling along the axis of the spray cone. The deceleration of fuel droplets is modeled by the conservation of momentum flux as described by Payri [11]. Directly downstream of the injector the momentum flux is $\dot{M}(0) = \dot{M}_0 = \dot{m} v_0$ where $\dot{m}$ is the rate of mass flow $\left[\frac{kg}{s}\right]$. After a traveled (axial) distance d the momentum flux is

$$\dot{M}_0 = \dot{M}(d) = \int_0^{R(d)} 2\pi r \cdot \rho(d,r) v^2(d,r) dr \tag{57}$$

where $R(d)$ is the width of the spray cone after a distance d and $\rho(d,r)$ is the fuel density at the position (d,r). The radial velocity distribution is assumed to be Gaussian:

$$v(d,r) = v_{axis}(d) \cdot e^{-\alpha\left(\frac{r}{R}\right)^2} \tag{58}$$

where R is the spray radius and α the shape parameter. In this work α is estimated by setting the radial distribution function equal to $\frac{1}{4}$ at the boundary of the spray cone giving $\alpha = -\ln\frac{1}{4} \sim 1.4$.

By also assuming a Gaussian distribution of fuel mass, constant Schmidt number and constant density equal to that of the surrounding gas a simple model for the axial velocity can be found [11]:

$$v_{axis} = \frac{\dot{M}_0^{1/2}}{\rho_f^{1/2}\left(\frac{\pi}{2\alpha}\right)^{1/2}\tan\left(\frac{\theta}{2}\right)\cdot d} \quad (59)$$

The model has by [11] been found to agree well with experiments performed at distances greater than 25 mm. Since the model gives $v_{axis} \to \infty$ as $x \to 0$ the model cannot be applied for too short distances. Also, the density ρ_f changes over time. The solution used in this work is to use the minimum value:

$$v_{axis} = \min\left(v_0\,, \frac{\dot{M}_0^{1/2}}{\rho_f^{1/2}\left(\frac{\pi}{2\alpha}\right)^{1/2} tan\left(\frac{\theta}{2}\right)\cdot d}\right) \quad (60)$$

3 Results

3.1 Qualitative dependence on parameters

The model was first tested for a fictive diesel engine case to see how the predicted evaporation depends on model parameters. The investigated parameters were fuel type (n-heptane or diesel/dodecane), mixing time curve (τ), heating rate (average diameter used for droplet heating) and the injector hole size (affects velocity). The time step size was set to 0.1 crank angle degrees (CAD) between -2 and 11 CAD and 1 CAD otherwise, where 0 CAD corresponds to the top dead center. One parcel was created per time step and the vaporization was calculated using a minimum of two sub steps per particle and parcel. The data used is summarized in All results presented for this case are averages of 40 cycles.

Table 1. Baseline case setup for parameter dependence investigations.

Engine data	
Fuel	diesel
Engine speed	2000 rpm
Bore	80 mm
Stroke	96 mm
Connecting rod	140 mm
Compression ratio	16.5
Mass of fuel	19 mg/stroke
Mass of air	480 mg/stroke
EGR mole fraction of initial gas	0.3

. A vaporization curve, a pressure trace and an optimized τ-curve was already made for this case. A guess for the injection curve was made by stretching and moving the vaporization curve to -2 and +5 CAD. All results presented for this case are averages of 40 cycles.

Table 1. Baseline case setup for parameter dependence investigations.

Engine data	
Fuel	diesel
Engine speed	2000 rpm
Bore	80 mm
Stroke	96 mm
Connecting rod	140 mm

Compression ratio	16.5
Mass of fuel	19 mg/stroke
Mass of air	480 mg/stroke
EGR mole fraction of initial gas	0.3
Engine speed	2000 rpm
Cylinder wall temperature	450 K
Number of injector holes	6
Spray angle	10°
Injector hole diameter	200 μm
Droplet average diameter D_{32}	2 μ
Droplet average diameter D_{43}	3 μm
Start of injection	-2 CAD
End of injection	2 CAD
Injected mass	20 mg
Simulation data	
Chemistry	n-heptane mechanism, 28 species and 58 reactions
Number of particles	200
Fuel properties used	diesel/dodecane
Number of cycles	40

3.1.1 Dependence on fuel type

Two calculations were made, one to simulate n-heptane and one to simulate diesel. The first calculation used only physical properties of n-heptane. For the second calculation, not all required data was available for diesel. The latent heat of vaporization, liquid heat capacity, liquid density, critical temperature and saturation pressure for diesel were taken from [10]; for vapor viscosity, vapor heat conductivity and vapor heat capacity values for dodecane taken from [10] and [12] were used, and for vapor diffusivity the n-heptane values were used. The result is shown in Figure 7 (total evaporated mass) and in Figure 8 (evaporation rate). It is evident that n-heptane evaporates faster than diesel fuel as expected. The main difference between the two is the higher critical temperature and lower saturated vapor pressure of diesel. The critical temperatures used were 540 K for n-heptane and 726 K for diesel [12].

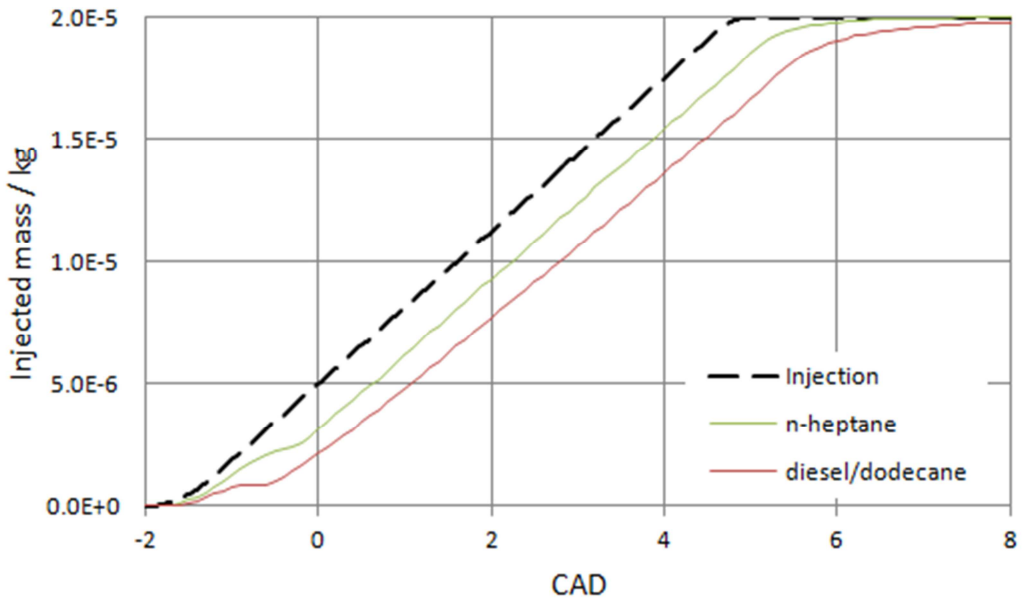

Figure 7. Injected and evaporated mass for calculations using fuel properties of n-heptane and diesel/dodecane.

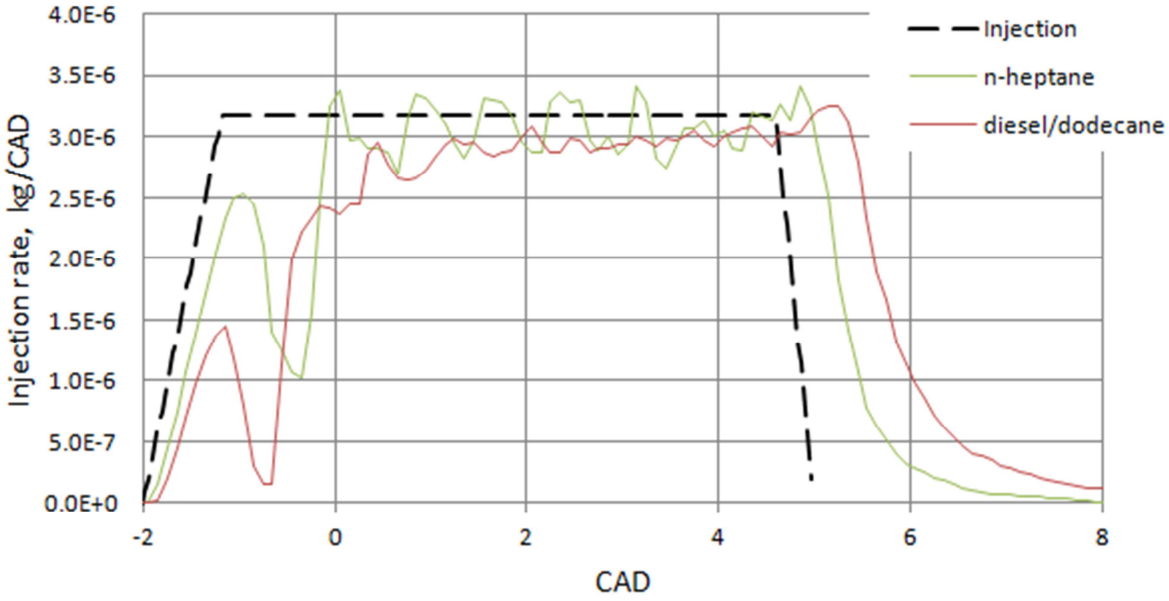

Figure 8. Evaporation rate for calculations using fuel properties of n-heptane and diesel/dodecane.

The evaporation rate shows a clear drop shortly after the start of injection. The explanation for this is that the first particle has been cooled and saturated so that no more fuel can evaporate in it, since that particle is longer than the others (it is the tip of the spray cone) it takes a little while before parcels have reached new particles where they can evaporate again. Inspection of the simulations confirmed that this is indeed what is happening. n-heptane is effected less because it does not require as high temperature as diesel to evaporate, thus it also takes a bit longer before low enough temperatures are reached.

Figure 10 shows a comparison of the diesel/dodecane calculation performed with 200 and 400 gas particles. The drop happens earlier with more (smaller) particles but this discretization error is only prominent in the beginning of the evaporation.

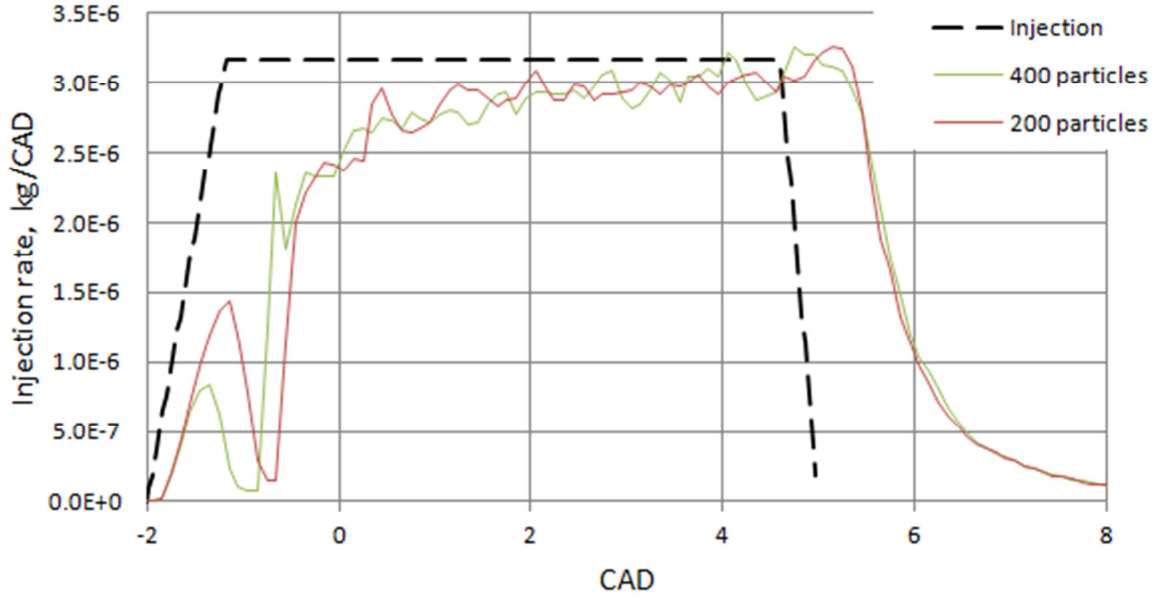

Figure 9. Evaporation rate calculation for diesel/dodecane using 200 and 400 gas particles.

3.1.2 Dependence on heating rate

The volume average diameter used to calculate the heat transfer rate was used as a free parameter and the calculation was performed using 0.5, 1, 2, 5 and 15 times the volume average. The result is shown in

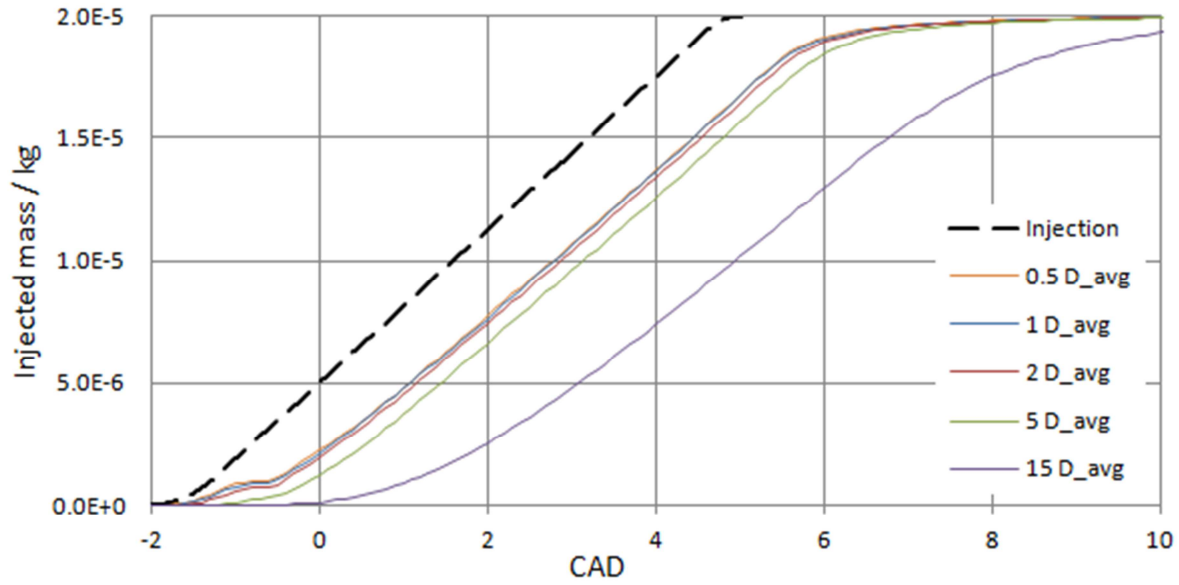

Figure 10. A larger diameter gives less area per volume, $\frac{A}{V} \propto \frac{1}{D}$, and thus slower heating and evaporation. The results shows that only large changes in the diameter (of the same order as the diameter itself) has any significant effect on the evaporation rate.

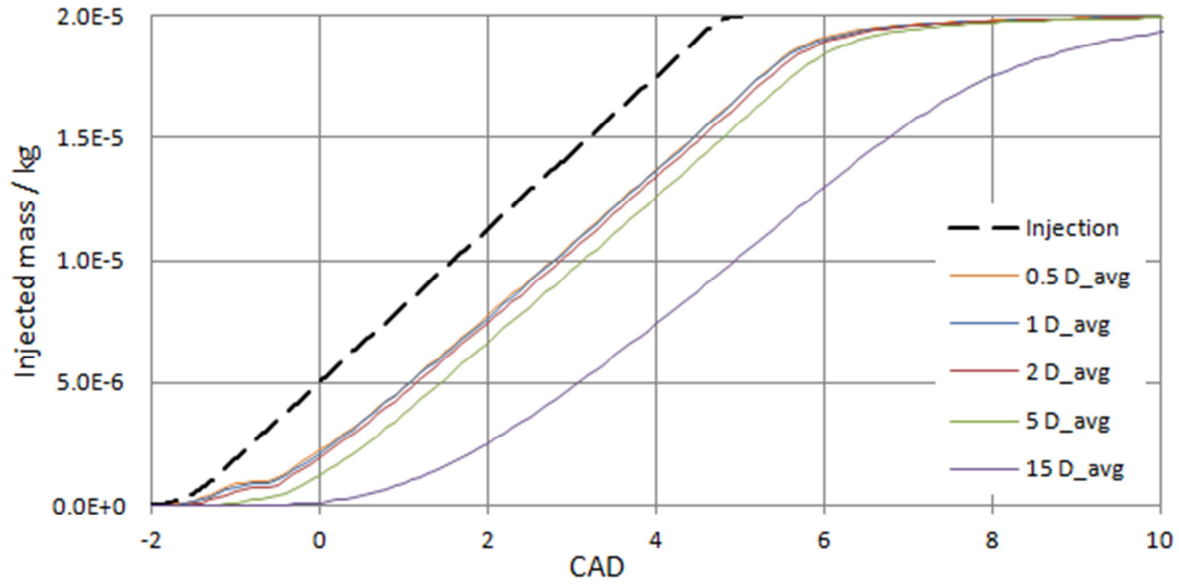

Figure 10. Evaporated mass using different multiples of the average diameter for the heating calculation.

3.1.4 Dependence on injector hole diameter

Smaller injector holes give faster droplets (with unchanged injection rate); the initial droplet velocity is inversely proportional to the injector area. Four diameters were compared: 130, 170, 200 and 230 µm corresponding to injector areas 0.08, 0.14, 0.19 and 0.25 $(mm)^2$ and maximum initial droplet velocities (for this injection rate and six injector holes) 570, 340, 240 and 180 m/s, respectively. The results are shown in Figure 11; lower velocity gives slower evaporation.

The level out of the curve noted in the fuel type investigation is even more visible here. It is barely present when the droplets have high velocities and quickly leaves the first particle but becomes longer as the droplets are made slower.

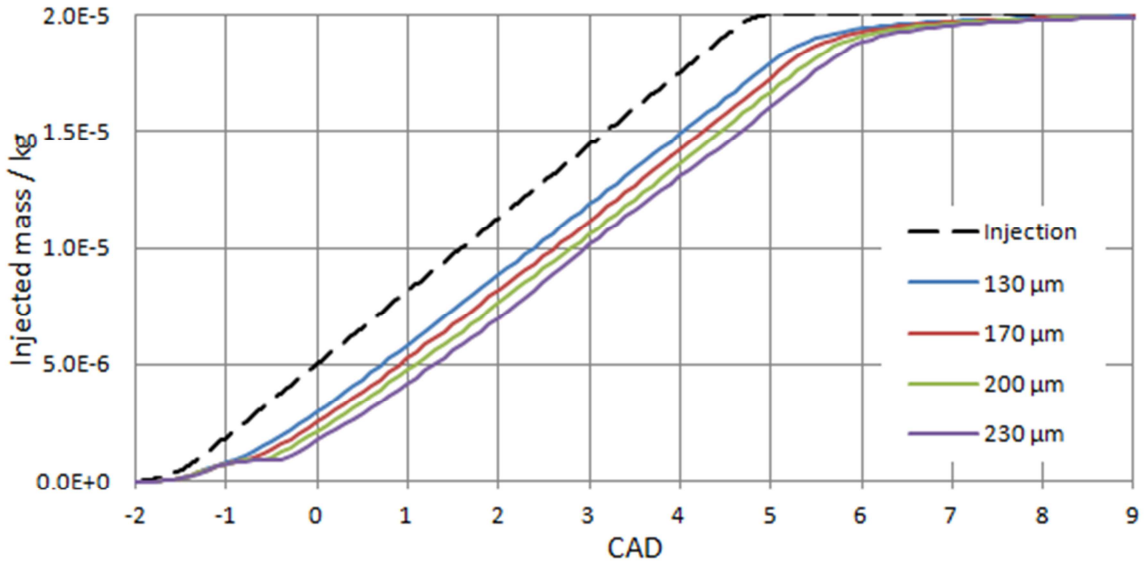

Figure 11. Evaporated mass with different injector hole diameters. Six injector holes were assumed.

3.1.5 Dependence on mixing time

The calculations were also performed for four different time-dependent mixing times (τ), see Figure 12. The original τ-curve is one that has been tuned to give a good fit to the pressure trace. The other three curves are modified versions of this; one is moved to later CAD, one has an increased minimum value and the last one has both these modifications. The resulting evaporated masses and evaporation rates are shown in Figure 13 and Figure 14. Tthe corresponding pressure traces are shown in Figure 15. It is worth pointing out that the assumed injection profile and the τ-curve does not match; the drop in τ between -1 and 0 CAD should correspond to the but the injection was set to start at -2 CAD (see the next section).

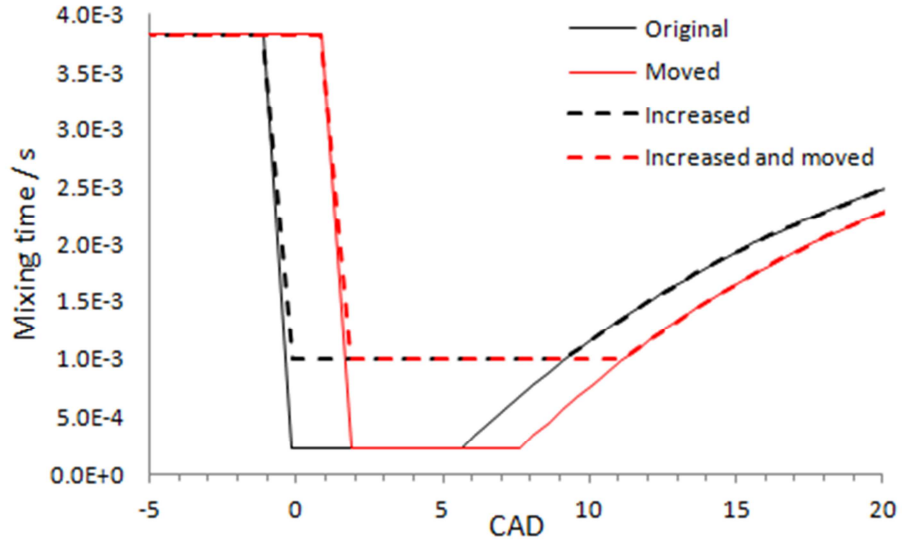

Figure 12. Original and modified mixing time curves.

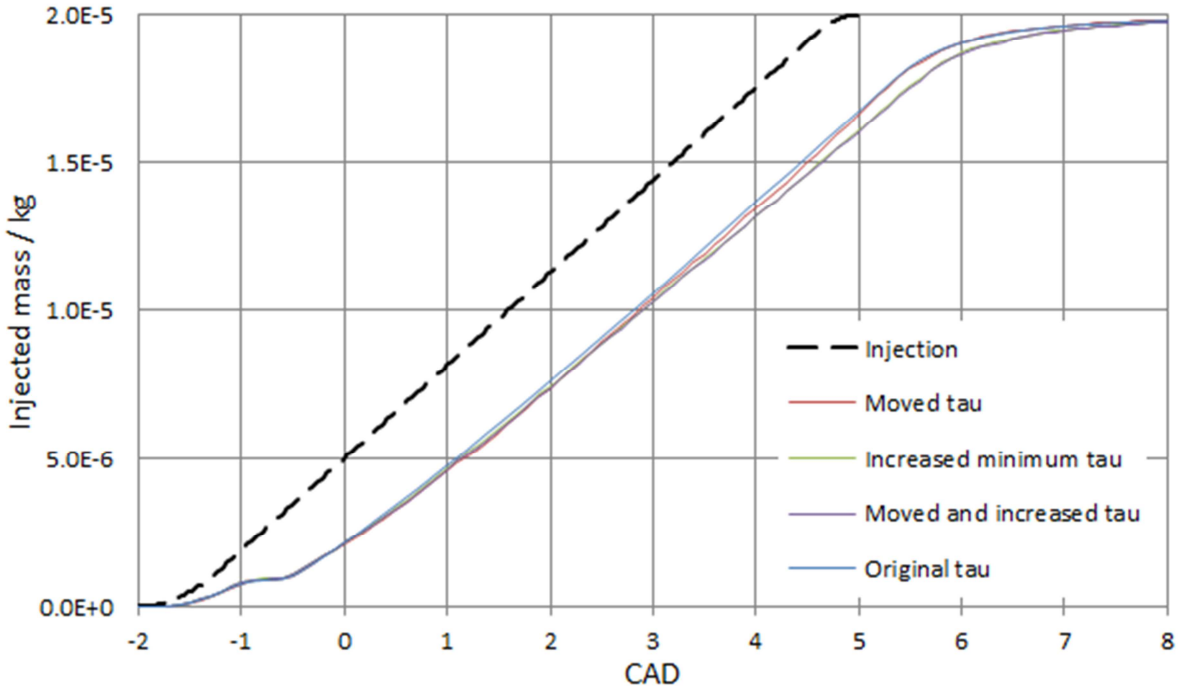

Figure 13. Evaporated mass for four different τ-curves.

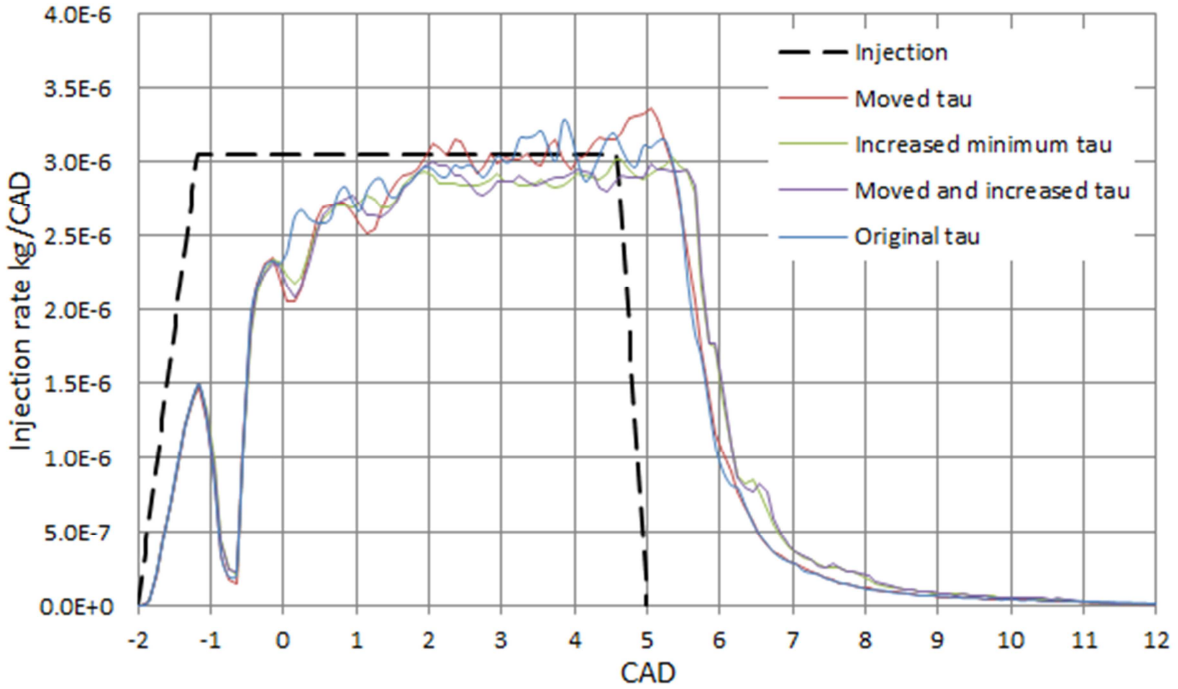

Figure 14. Evaporation rate for four different τ-curves.

The evaporation does not differ significantly between these τ-curves. This means that the mixing, and thus the saturation and cooling of particles, is not the limiting factor for the evaporation rate. It may be explained by the parcels moving through the particle queue so fast

that the particles does not become saturated and cooled enough to limit the evaporation (with exception for the very first particle, see the section about fuel type dependence). However, the combustion is gratefully affected as shown by the pressure traces. A changed τ-curve delays the ignition and may significantly lower the pressure peak. For a discussion of the dependence on τ, see for example the work by Mario Morgalla [14].

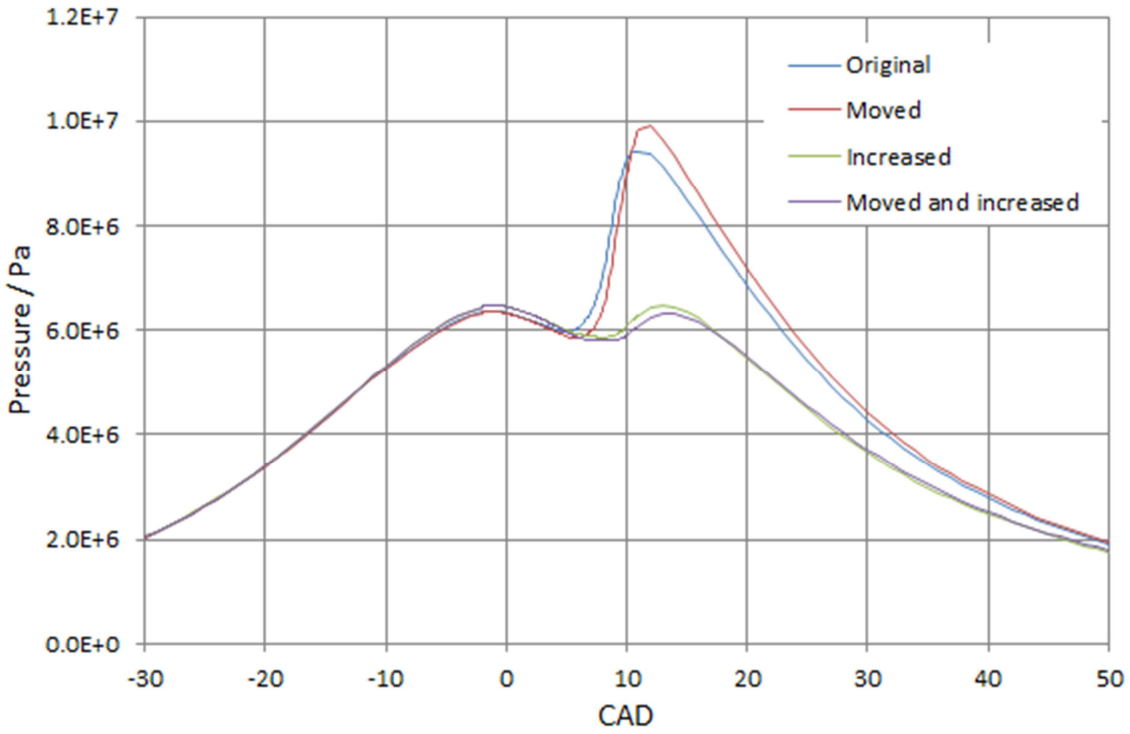

Figure 15. Pressure trace for different τ-curves.

3.2 Constructing an injection profile

The injection curve used for the parameter studies was just a guess, however, a more reasonable injection curve can be constructed using the optimized τ-curve. τ represents the level of turbulence in the cylinder which, during injection, is dominated by the spray. An injection curve can thus be constructed by moving and stretching the vaporization curve to place it on the interval where τ is minimal.

The start of the injection is clearly where the sharp drop in τ begins but the end of injection is not as clear. Three different injection curves constructed in this way are shown in Figure 16 together with the τ-curve and the fitted vaporization curve. The computed evaporation for these injection curves is shown in Figure 17 and the corresponding pressure traces in Figure 18. As expected from the longer injection time and the study of velocity dependence, slower injection gives later evaporation.

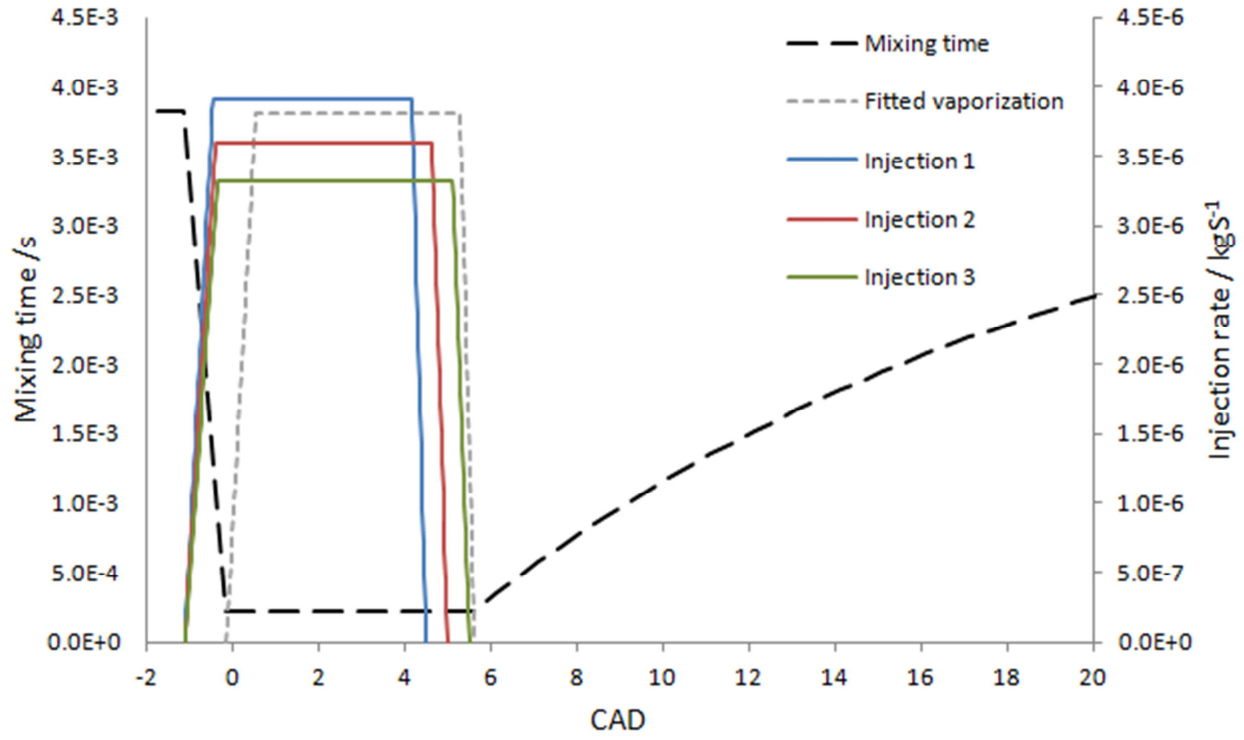

Figure 16. Three different constructed injection curves and the τ-curve.

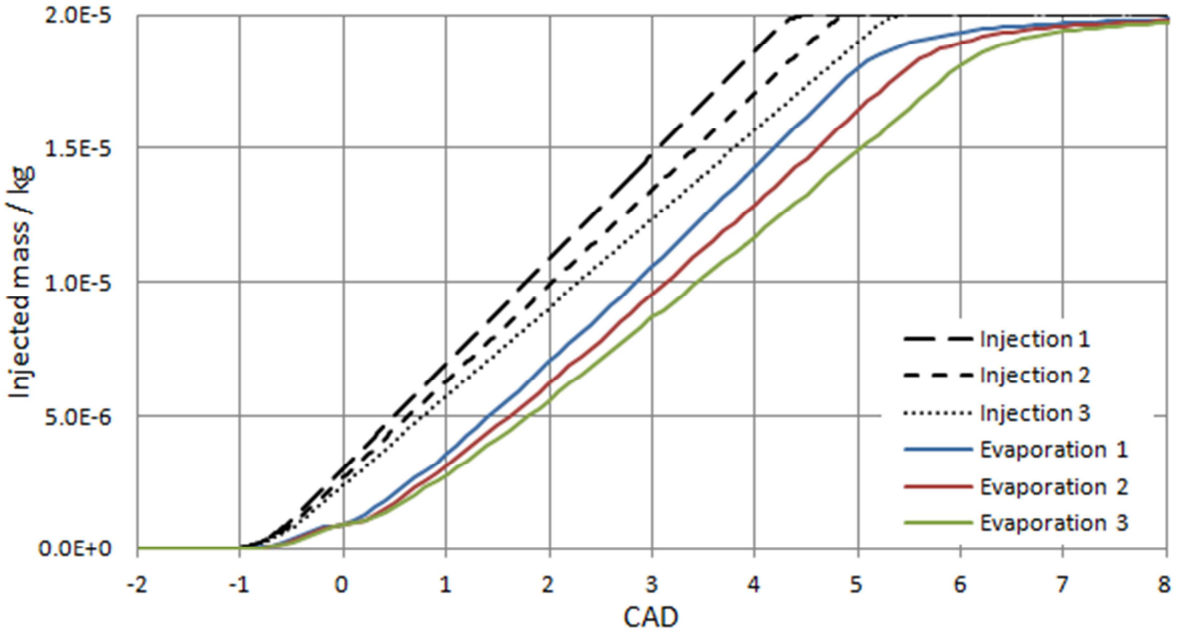

Figure 17. Evaporated mass for three different injection profiles.

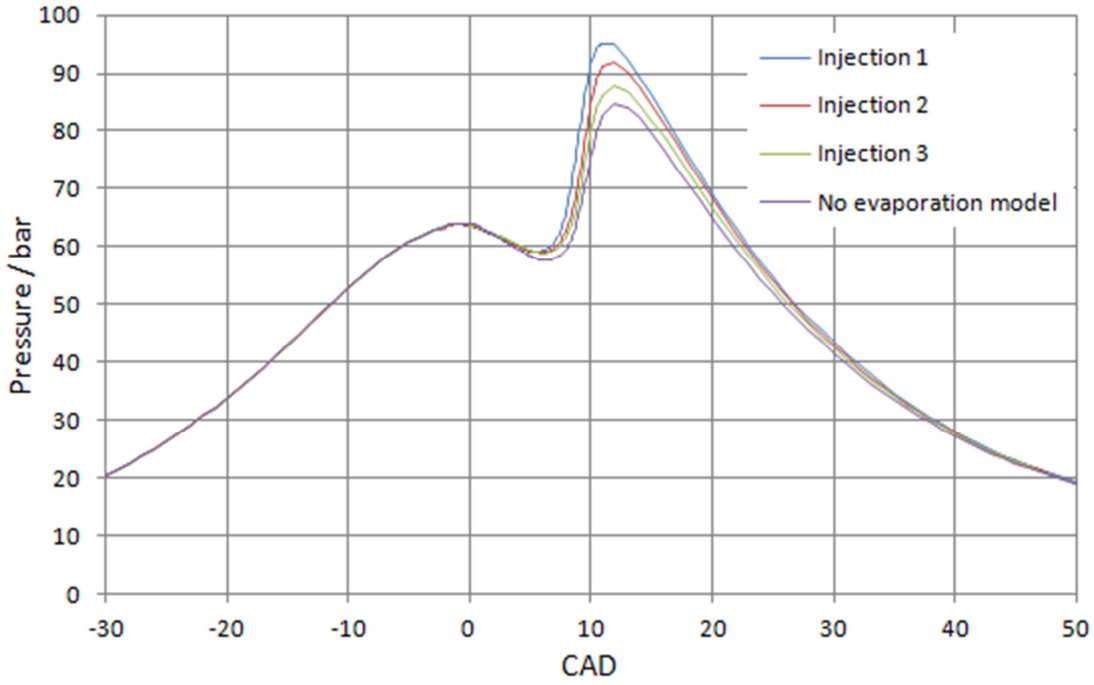

Figure 18. Predicted pressure trace using three different injection profiles for the evaporation model and for a calculation without the evaporation model using a fitted evaporation curve.

3.3 Comparison with an experimental case

The model was also tested with an experimental case in which the engine had been fuelled by actual n-heptane; this was the same case as used by Morgalla [14]. This should minimize the error introduced by using the diffusivity of n-heptane instead of diesel and by using n-heptane as surrogate fuel in the chemistry. As n-heptane is much more volatile than diesel, the delay between injection and evaporation is small, so fast evaporation is expected.

The real injection profile was not available in this case so the same method as described above was used to construct an injection curve from the fitted evaporation and τ-curves, see Figure 19. The data used in the simulation is summarized in Table 2. The calculation was run both with the evaporation model and with the fitted evaporation curve. The evaporation and pressure curves are shown in Figure 20 and Figure 21, respectively, the results are averages of 25 cycles.

Table 2. Baseline case setup for comparison with experimental case.

Engine data	
Fuel	n-heptane
Engine speed	2000 rpm
Bore	81 mm
Stroke	95.5 mm
Connecting rod	144 mm
Compression ratio	16.3
Injected mass	17.2 mg
EGR mole fraction of initial gas	0.329
Cylinder wall temperature	450 K
Number of injector holes	6*

Spray angle	10° *
Injector hole diameter	200 µm*
Droplet average diameter D_{32}	2 µm*
Droplet average diameter D_{43}	3 µm*
Start of injection	-0.5 CAD*
End of injection	4.7 CAD*
Simulation data	
Chemistry	n-heptane mechanism, 121 species and 973 reactions
Number of particles	200
Fuel properties used	n-heptane
Number of cycles	25

* These parameters are only estimates.

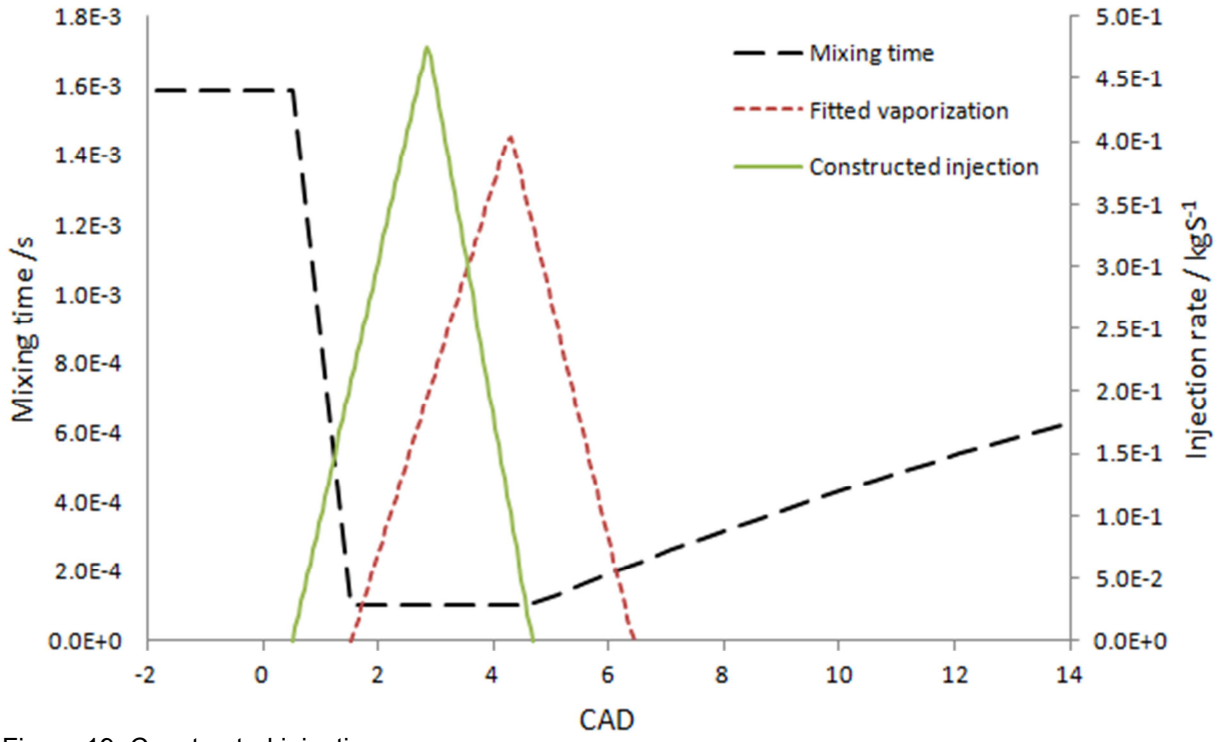

Figure 19. Constructed injection curve.

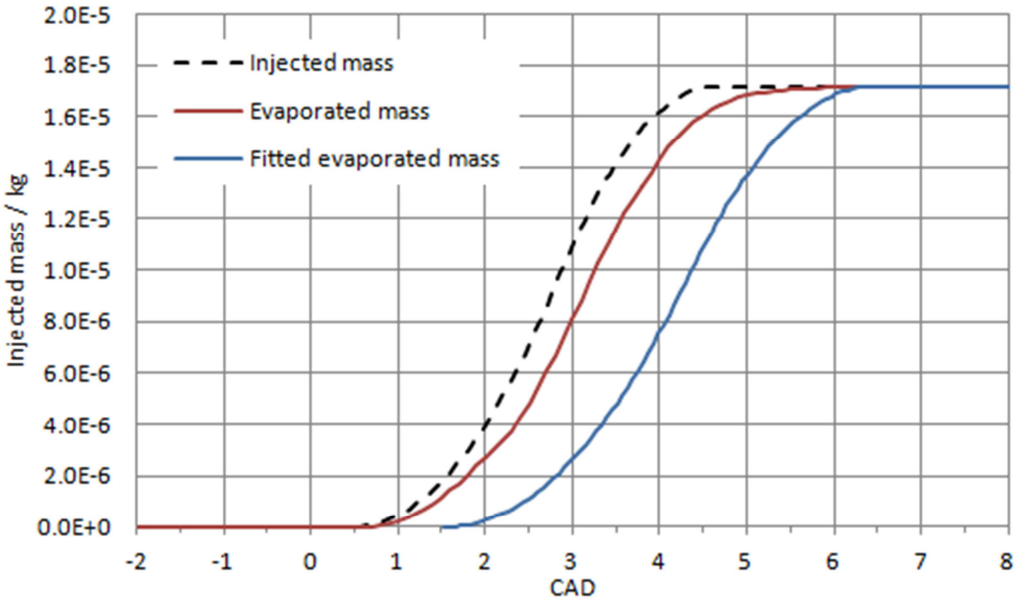

Figure 20. Injection and evaporation for the first run of the n-heptane case.

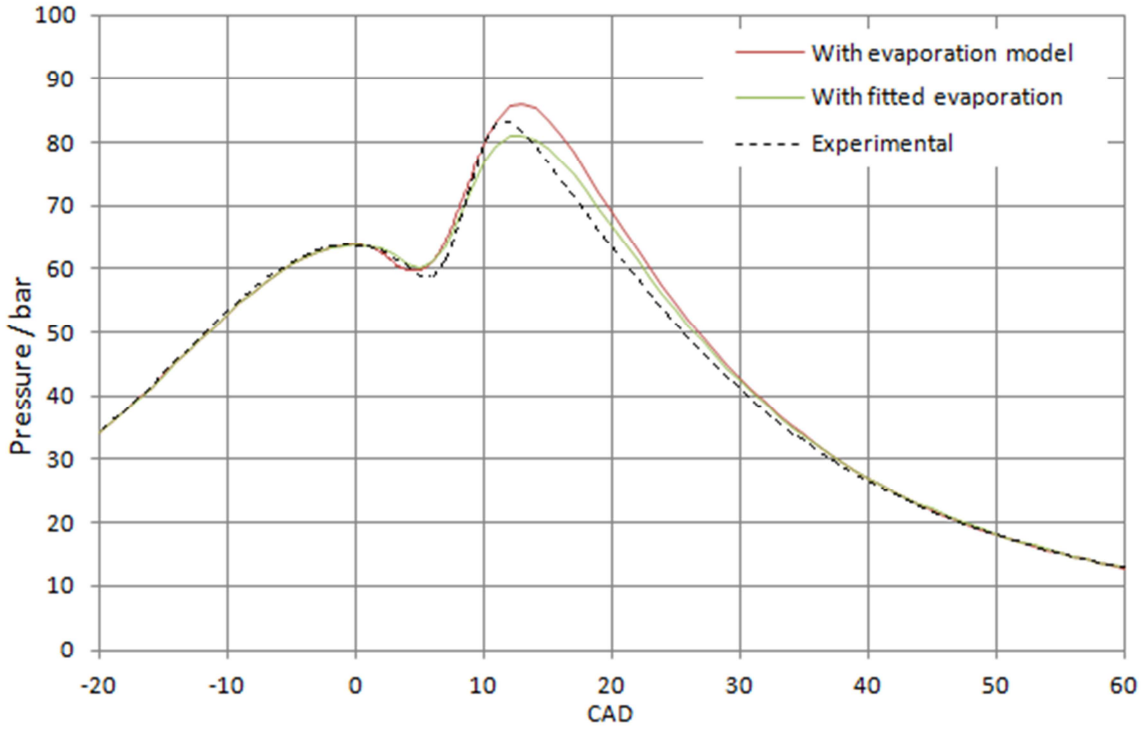

Figure 21. Pressure trace for the first run of the n-heptane case.

Since the first run predicted only a small delay between injection and evaporation compared to the fitted curve, a second run was made with slightly different settings that should result in a longer delay. The injection was set to start at the same point but was stretched to end 1 CAD later, the injector hole diameter was increased to 220 µm and the mean diameters D_{43} and

D_{32} were changed to 4 µm and 3 µm respectively. This resulted in the more delayed vaporization curve shown Figure 22 and Figure 23. Figure 24 shows the corresponding pressure trace. The accumulated heat release is shown in Figure 25 and the heat release per CAD is shown in Figure 26.

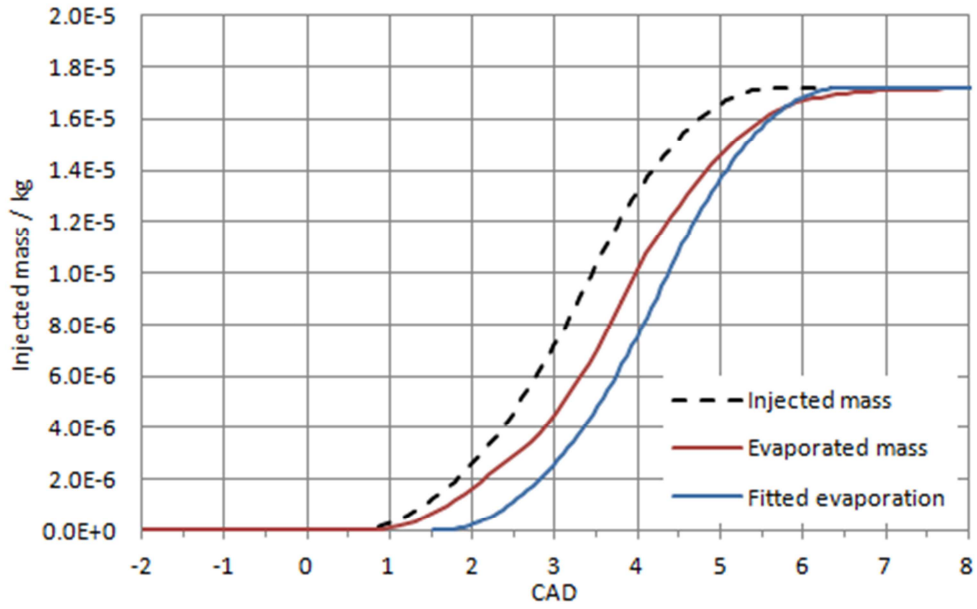

Figure 22. Injection and evaporation in the second run of the n-heptane case.

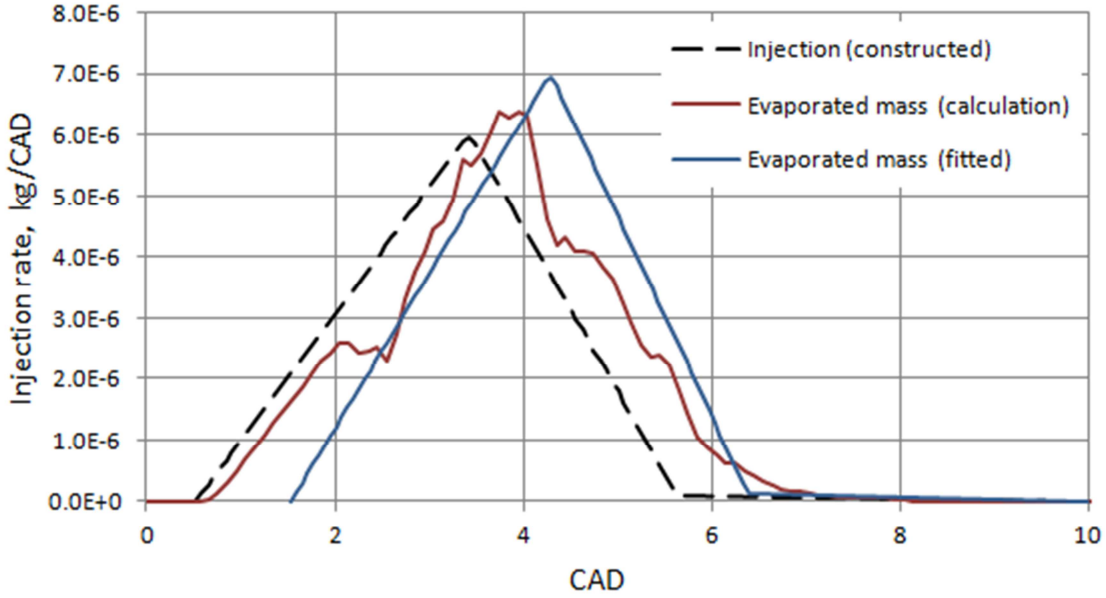

Figure 23. Injection and evaporation rate in the second run of the n-heptane case.

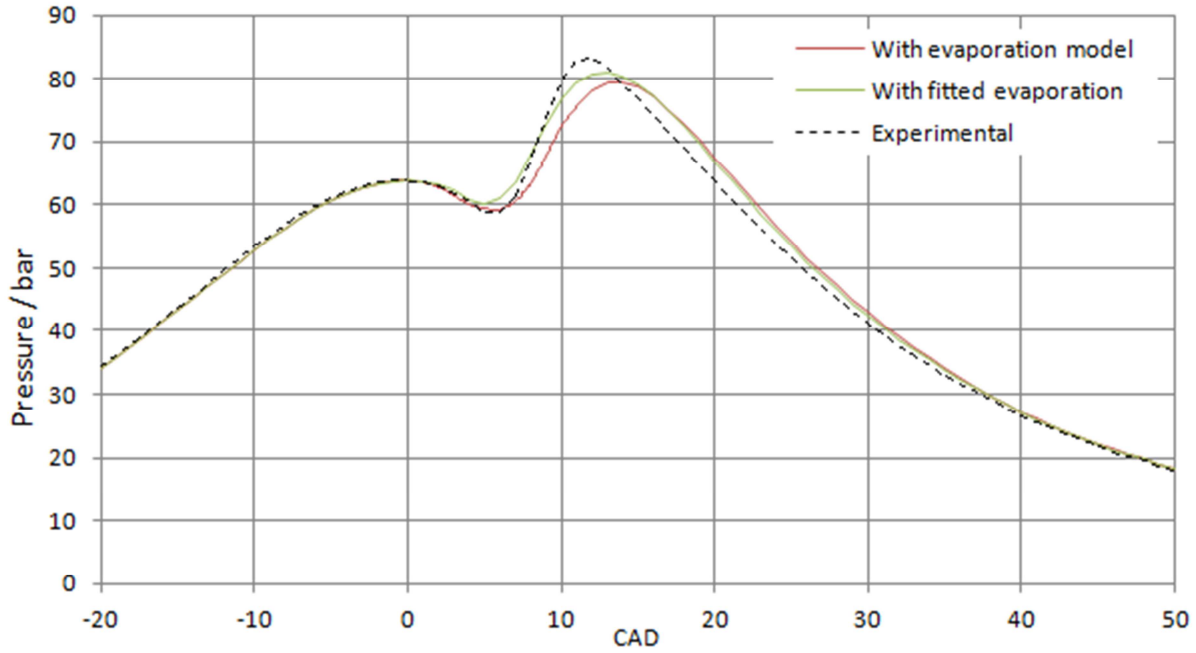

Figure 24. Pressure trace for the second run of the n-heptane case.

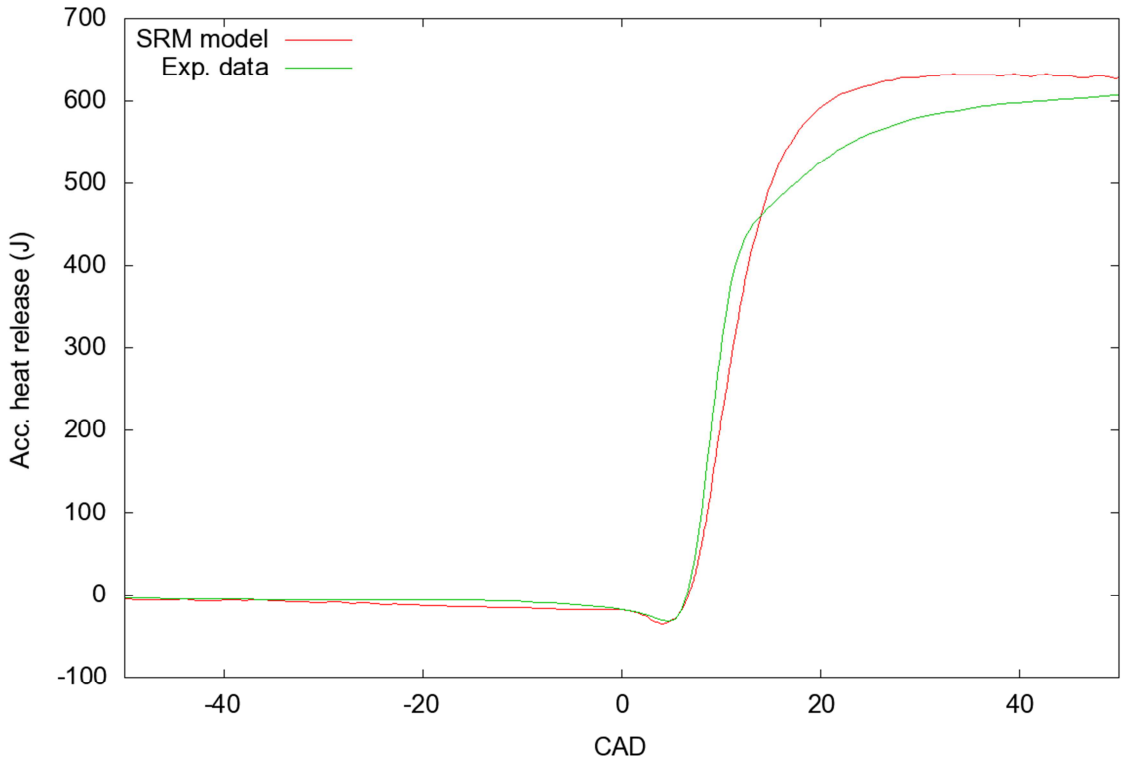

Figure 25. Accumulated heat release for the second run of the n-heptane case.

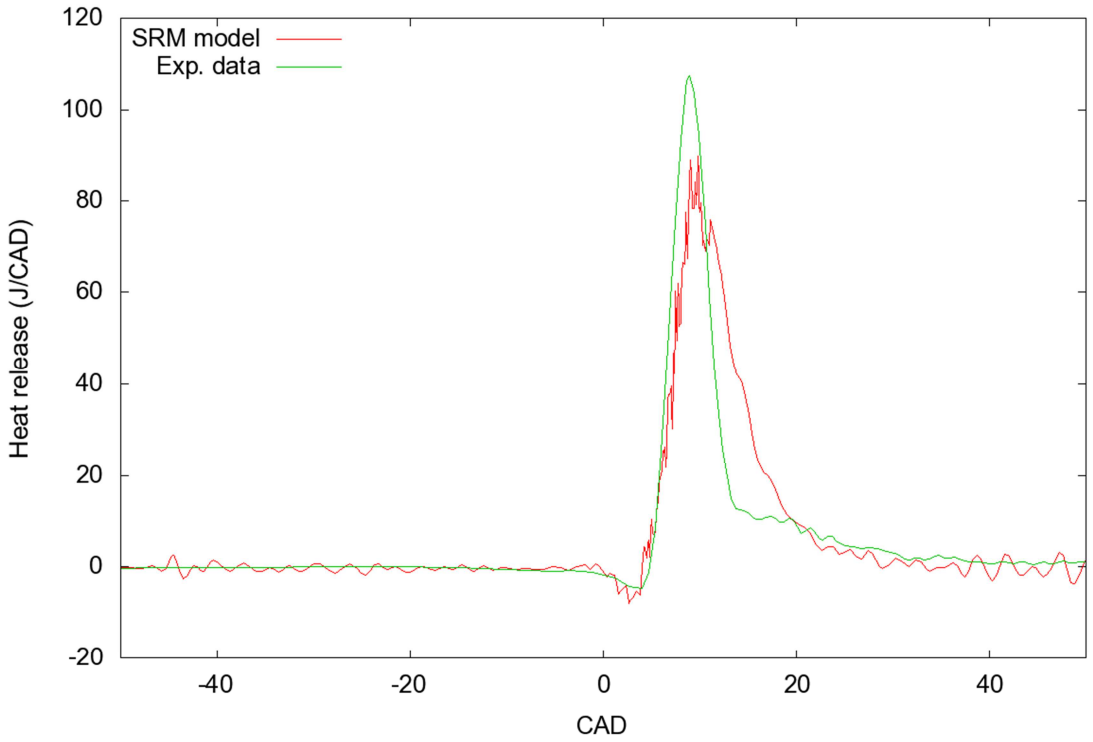

Figure 26. Heat release per CAD for the second run of the n-heptane case.

The vaporization in the second run agrees better with the fitted vaporization curve than that from the first run does. It is also less steep as a result of slower evaporation due to the larger and slower droplets. As seen in the investigation of injector hole size, slower droplets tend to just move the evaporation curve to a later CAD, so the decreased slope is probably an effect mainly of the larger droplets.

The heat release shows a quite good agreement in ignition timing but the combustion is a bit too slow. This is probably an issue with the τ-curve being optimized for another fuel injection model that distributes the fuel in a different way.

4 Conclusions

A vaporization model has been developed and implemented into the DARS SRM code and tested. The dependence of evaporation rate on fuel type, heating rate, injector hole size and mixing time has been investigated for a diesel case. The model has also been tested with an experimental n-heptane case.

The n-heptane case may not be ideal for testing the vaporization model because the vaporization is so fast; it is not possible to see if the model under-predicts the evaporation time, so further testing and validation ought to be done with less volatile fuels to check this. However, most of the sub-models used are not new to this work but has been applied before and the results look qualitatively reasonable.

What is less obvious is how well the model work together with the SRM code and its stochastic particles. The gas flow and turbulence in an engine cylinder is a complex phenomenon which the SRM simulates indirectly by the stochastic mixing of particles governed be the time-dependent mixing time. The mixing of particles affect the evaporation by changing the surroundings of the spray, but as seen in Figure 13 the effect of changing the mixing time on the

evaporation is very small compared to the effect on the pressure trace. This means that the evaporation model is quite stable as it does not start to misbehave as the τ-curve is tuned, indicating that it should work quite well with the SRM. However, the τ dependence should be more pronounced if the droplets are slower. It should also be more pronounced if fewer particles are used; the model has to use a sufficient number of particles. The weak dependence on τ came a bit unexpected; the increased minimum value of τ should result in the particles representing the first part of the spray cone becoming cooler and more saturated which gives slow evaporation. Probably the droplets were just so fast moving that cooling and saturation didn't have any significant effect.

The average diameter used for heating calculation was kept as a parameter to allow the heating model to be tuned independently of the evaporation/diffusion calculation. This tuning might be needed because the temperature is assumed diameter-independent but and also because the volume average diameter may not be the most representative one to use. The investigation of this mean diameter (Figure 10) shows that this dependence is weak; the diameter must be more than doubled/halved to introduce any significant change.

It is crucial for the evaporation model to work that the properties of liquid fuel and fuel vapor used are for the correct (or a similar) fuel. The difference in injection/vaporization delay between n-heptane and diesel/dodecane is significant; it is in general not possible to use the same surrogate fuel for evaporation as for the chemistry. Another point about fuel types is that the separation of calculations for different fuel components in multi-component fuels allows the components to evaporate at different rates and may predict separation the components and different component concentrations in different parts of the cylinder gas.

The dependence on injector hole diameter and velocity is clear; a smaller injector hole gives faster droplets that interact with more particles reducing the effects of cooling and saturation of particles.

The test with the n-heptane case gave a fairly good agreement between the pressure traces calculated with the estimated vaporization curve and the vaporization in the second attempt. The predicted vaporization curves were qualitatively different between the two attempts compared to the estimated curve; the second one was not as steep, probably as a result of the injection curve being stretched.

The flattening of the evaporation curve observed in the beginning of the evaporation in cases where the droplets are relatively slow was concluded to be an effect of saturation and cooling of the first particle which is also longer than the other particles in the spray cone; it takes time for droplets to leave the first particle. Part of this effect may be a discretization error which can be avoided by using a larger number of particles, but some of it could be a real physical effect of the first part of the spray cone interacting only with a small volume of gas.

When it comes to the τ-curve no new tuning was done in this work, but the τ-curve already tuned for use with the estimated evaporation curve was used. Since τ represents the turbulence in the cylinder, its qualitative shape should be similar regardless of whether or not the vaporization model is used. However, the numerical values on the curve may differ because τ was tuned for an injection model which distributes the fuel among particles in a completely different way than the vaporization model. This is expected to introduce differences in ignition timing and early burn rate because of the different fuel distributions.

A sensitive part of the model is the separation of evaporation and heating. The evaporation is calculated before the heating so the effect of the separation is slower evaporation. The shorter the time step is the smaller is this effect. The "global" time step is thus a limiting factor, but in

cases where the droplets travel through more than one particle per step the evaporation and heating calculations are performed once per particle and thus not directly limited by the global time step but instead by the number of particles (it is still dependent on the time step indirectly since the rest of the model, including mixing, depends on that). Thus the accuracy of the evaporation and heating calculations depends on the number of particles and the time step. It is advisable to use shorter global time steps during the evaporation process, but in cases where this wants to be avoided due to some other parts of the simulation being very time consuming the vaporization calculation can instead be done in using shorter sub-steps independent of the rest of the simulation.

5 Future work

So far the model has just been tested with one real case for which only limited data on the injection is available, which limits the conclusions that can be made about the validity of the model. To determine the range of validity or invalidity some more extensive testing and of the model has to be made using cases with known injection curves, this may be either experimental cases or three-dimensional CFD calculations. The model could also be applied to a case with multi-component fuel and the separation of the fuels in the cylinder gas investigated.

Two important extensions that can be made is to let droplets of different size in the same parcel have different temperature and the development of a wall wetting model. The former may for example be achieved by dividing each parcel into a small set of size classes based on the distribution of mass and treat the size classes independently. Other extensions could be to calculate the injection rate based on injector pressure, geometry and the electrical signals, to make the spray cone two-dimensional (include radial as well as axial position of droplets) and to keep heating parcels above the critical temperature by changing to gas properties instead of liquid properties.

Some more elaborate work would be to develop a method to predict the τ-curve based on the spray parameters and piston movement.

6 References

[1] ”DARS manual,” i *Book 3 - Engine in-cylinder reactor models*, DigAnaRS LLC., 2012.

[2] A. De´chelette, E. Babinsky och P. Sojka, ”Drop Size Distributions,” i *Handbook of atomization and sprays*, Springer Science, 2011, pp. 479-495.

[3] K. K. Kuo, Principles of combustion, New York: Wiley, 1986.

[4] F. Tanner, ”Evaporating Sprays,” i *Handbook of atomization and sprays*, Springer Science, 2011, pp. 263-278.

[5] S. R. Turns, An introduction to combustion, McGraw-Hill Book Co, 2000.

[6] J. J. Karlsson, Modeling auto-ignition, flame propagation and combustion in non-stationary turbulent sprays, Göteborg: Chalmers universty of technology, 1995.

[7] R. Bird, Transport Phenomena, Wiley, 2007.

[8] P. Incropera, Fundamentals of heat and mass transfer, Notre Dame: Wiley, 2007.

[9] G. Anand, ”Stochastic modeling of evaporating sprays within a consistent hybrid joint PDF

framework,” Journal of computational physics, 2009.
[10] E. Wakil, ”A theoretical investigation of the heating-upperiod of injected fuel droplets vaporizing in air,” 1954.
[11] R. Payri, ”Spray droplet velocity characterization for convergent nozzles,” 2008.
[12] S. Sazhin, ”Advanced models of fuel droplet heating and evaporation,” 2005.
[13] N. i. o. s. a. technology, ”NIST Chemistry WebBook,” 29 March 2012. [Online]. Available: http://webbook.nist.gov/chemistry/. [Använd 8 May 2012].
[14] M. Morgalla, ”Engine Simulations using a Stochastic Reactor Model,” BTU Cottbus, Cottbus, 2011.
[15] M. M. F. L. F. S. S. H. E. M. A. Pasternak, ”Simulation-Based Fuel Testing for Diesel Engine,” European Combustion Meeting, Cardiff, UK, June 2011.
[16] S. Sazin, ”Models for fuel droplet heating and evaporation: Comparative analysis,” University of Brighton, Brighton, 2006.
[17] W. A. Sirignano, Fluid Dynamics and Transport, 1999.